THESIS ON NATURAL AND EXACT SCIENCES B106

Sea Ice Deformation Events in the Gulf of Finland and Their Impact on Shipping

OVE PÄRN

TUT
PRESS

Marine Systems Institute
TALLINN UNIVERSITY OF TECHNOLOGY

Doctoral dissertation was accepted for the commencement of the degree of Doctor of Philosophy in Natural Sciences on April 13, 2011

Supervisors: Prof. Jüri Elken, Marine Systems Institute at Tallinn University of Technology, Estonia

Dr. Jari Haapala, Finnish Meteorological Institute, Finland

Opponents: Prof. Pentti Kujala, Aalto University School of Science and Technology, Finland

Prof. Jaak Jaagus, Faculty of Science and Technology at the University of Tartu, Estonia

Defence of the dissertation: June 20, 2011 at the Marine Systems Institute at Tallinn University of Technology, Akadeemia tee 15, Tallinn, Estonia

Declaration:

Hereby I declare that this doctoral dissertation, my original investigation and achievement, submitted for the doctoral degree at Tallinn University of Technology has not been submitted for any degree or examination.

/Ove Pärn/

ISSN 1406-4723
ISBN 978-9949-23-089-1 (publication)
ISBN 978-9949-23-090-7 (PDF)

LOODUS- JA TÄPPISTEADUSED B106

Merejää deformatsioonid Soome lahes ning nende mõju laevaliiklusele

OVE PÄRN

TTÜ
KIRJASTUS

Contents

LIST OF PUBLICATIONS

This dissertation is based on the following papers, which will be referred to in the text by their Roman numerals.

I. Pärn, O., Haapala, J., Kõuts T., Elken J. & Riska, K. 2007. On the relationship between sea ice deformation and ship damages in the Gulf of Finland in winter 2003. *Proc. Estonian Acad. Sci. Eng*., 13, 201–214.

II. Pärn, O. & Haapala, J. 2011. Occurrence of synoptic flaw leads of sea ice in the Gulf of Finland. *Boreal Environ. Res.*, 16(1), 71–78.

III. Pärn, O., Haapala, J. & Sipelgas, L. 2010. Leads as natural fairways in the Gulf of Finland. Baltic International Symposium (BALTIC), 2010 IEEE/OES US/EU, 1 – 7, doi: 10.1109/BALTIC.2010.5621638

1. INTRODUCTION

1.1. Background

The Gulf of Finland (Figure 1) is characterized by a unique combination of extensive seasonal ice cover and high shipping intensity. Owing to the maritime transport, historical data of ice observations carried out in Tallinn port extend back for more than 500 years from now (Tarand and Nordli, 2001). Based on the data from the Automatic Identification System (AIS) for monitoring the maritime traffic in the Baltic Sea area in 2006, more than 37 000 larger ships over 300 GRT enter or leave the entrance line of the Gulf of Finland annually (HELCOM, 2006; paper I). Analysis of shipping safety shows that a considerable part of the accidents are caused by "tough ice conditions" (Kujala *et al*., 2009).

The Gulf of Finland is a narrow, shallow and ecologically vulnerable sea area of the Baltic Sea. It is about 400 km long and its width varies between 60 and 135 km, whereas there are a large number of underwater rocks in the Finnish Archipelago area. The eastern part of the Gulf of Finland is fully ice covered in normal and severe winters, while a few of its areas freeze even in very mild winters. The thickness of the ice varies following the differences in the age of the ice and the various processes how the main ice types form.

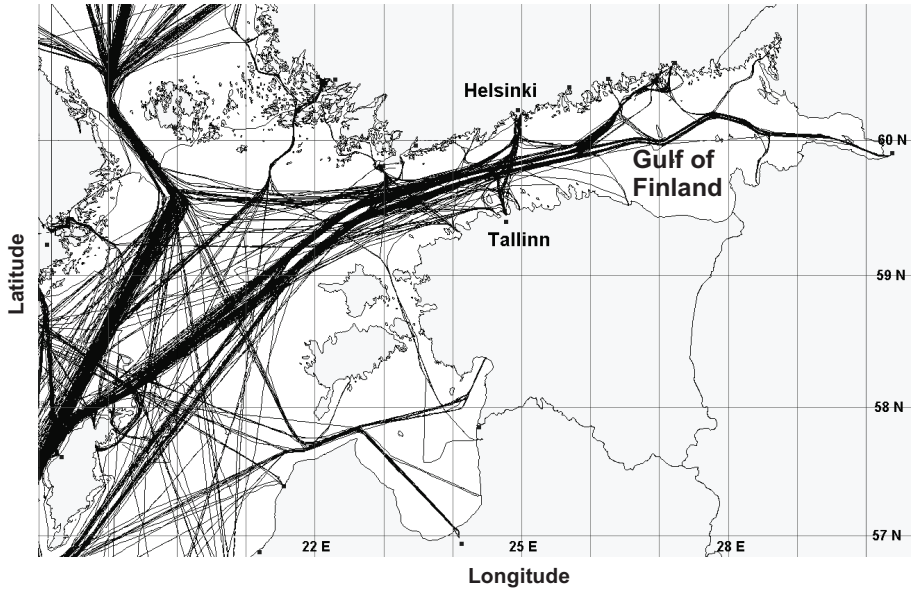

Figure 1. Map of the Gulf of Finland in the northeastern Baltic Sea. The selected ship routes from the first half of April 2007 are shown by the HIROMB-SeaTrackWeb data (Swedish Meteorological and Hydrological Institute; the routes not necessarily represent the long-term shipping statistics).

The sum of negative degree-days and winds affect the ice conditions in the Gulf of Finland. The winds control the drift and ridging events on the ice field, also opening leads in pack ice. Openings in ice are a common feature in the Gulf of Finland. If a lead emerges along the Gulf of Finland axis, it facilitates the navigation through the area.

Sea-ice conditions differ strongly in the east–west direction. At first, ice forms in the eastern part of the gulf already at the beginning of December and it melts there usually in the middle of April (Jevrejeva *et al.*, 2004). The coastal current from the Baltic Proper and the southern to southwestern winds together keep the southern part of the Gulf of Finland relatively ice free.

The coastal morphology causes a wide fast ice zone along the northern fragmented coast with many small embayments and islands, creating an asymmetry of ice conditions with the more open southern coast. The average date of permanent ice cover formation in the Gulf of Finland estuary is February 10, whereas the ice disappears from the gulf during mid-April (Seinä and Peltola, 1991). Ice cover lasts longer in the eastern part of the Gulf of Finland and shorter in its estuary. The average amount of ice days varies from ca 20 in the southern part of the open gulf and ca 60 in its northern part to up to 120 in a few coastal bays in the eastern part of the gulf (paper II). In severe winters the ice cover duration is respectively 40–100 and 140 days (paper III).

The level ice in the Gulf of Finland is typically 30–40 cm thick, but under certain snow-free conditions it may thermally grow up to 90 cm thick (Seinä and Peltola, 1991).

Near the shore, there are landfast ice areas, which persist during the most of the ice season. The width of such a durable landfast ice area depends on the bottom topography: islands and grounded sea ice ridges provide supporting points to stabilize the ice sheet. In the Gulf of Finland, the grounded ridges have such size that the landfast ice edge lies somewhere near the 10 m isobaths (Leppäranta, 1981).

A dynamic drift ice cover forms in the middle of the Gulf of Finland and elsewhere away from the shores, the islands and the shoals. A floe may vary from 10 m to 10 km in size. Drift ice appears as a long narrow field. It is dynamically sensitive to its compactness and thickness. Also the wind direction affects considerably the drift ice field (Soomere *et al*., 2008).

The mechanical behavior of drift ice varies strongly depending on its compactness. Open ice behaves as a frictionless medium; the moderately compacted ice seems to be a viscous fluid; highly compacted ice behaves as an elastic–plastic plate (Leppäranta, 2005).

The pack ice in the gulf tends to raft and ridge frequently – the portion of ridged ice extends usually to 25% in February (Swedish Meteorological and Hydrological Institute, 1982). Ice thickness measurements in the Baltic Sea (Similä *et al*., 2006) have shown that the amount of deformed ice is significantly larger than reported in the routine ice charts, and the mean ice thickness (taken over several square kilometers) could exceed consequently 2–3 meters in large

areas of the Baltic Sea. The largest observed ridges were 6–8 m thick (Leppäranta and Hakala, 1992), but it is probable that larger ones exist, perhaps in the eastern part of the gulf near the fast ice boundary at Kotka–Viipuri longitudes (Leppäranta and Wang, 2002).

In the Baltic the visible part of the ridge, the sail, is typically 1–3 m high while the bulk of the ridge volume is contained in the 5–15 m deep subsurface keel (Lensu, 2003). Such ice structures seriously endanger a vessel navigating among the sea ice. The probability of navigation disasters is rising in areas with high deformed ice growth rate (Palosuo, 1975; paper I).

The increasing shipping activity in the Gulf of Finland has raised concerns about the safety of maritime traffic. For example, during the severe winter of 2002/2003, ca 62% of ship hull damages over the Baltic Sea occurred in the Gulf of Finland. Some 30% of the damages were caused by ship–ice interaction and 15% of them occurred in a compressive ice field (Hänninen, 2003). An illustration of a ship collision in the ice field is given in Figure 2.

Figure 2. The MS *Yevgeniy Titov* collides with the MS *Bremer Saturn* in the Gulf of Finland, February 2003.

Various international and regional policy instruments aim at minimizing the risks of accidents and other harmful effects of shipping (Kuronen and Tapaninen, 2009). Much attention is paid to navigation safety, especially with respect to winter navigation, at both the scientific and management levels with seriously considering many environmental concerns (HELCOM, 2007; Kuronen and Tapaninen, 2009).

A number of authors have studied historical ice conditions in the Gulf of Finland (Leppäranta and Seina, 1985; Jevrejeva *et al*., 2004; Jaagus, 2006), focusing on climatological aspects of fast ice. Mechanical behavior (including drift) of pack ice fields is another direction of ice studies, reviewed by Leppäranta (2005) and Leppäranta and Myrberg (2009). Leads as open water areas between pack ice and fast ice have been extensively studied in the Arctic Ocean (Zakharov, 1996; Dethleff *et al*., 1998; Liu *et al*., 2009). In the Gulf of Finland, weather-dependent synoptic flaw leads are often observed on routine ice charts and remote sensing images, but they have not been widely analyzed in scientific publications. Haas (2004) carried out detailed ice thickness measurements along the Finnish Baltic Sea coast in February 2003 by using the helicopter-borne electromagnetic-inductive (HEM) method. The lead detected in the Gulf of Finland was surrounded with thick deformed ice (up to 5 m) between Helsinki and Tallinn. The HEM results confirmed that routine ice charts can be used for historical analysis of ice leads. Kortovirta *et al.* (2009) recently built a prototype system for ship route optimization in ice-covered waters of the Gulf of Bothnia, using dynamic (time-variable) ice information and ship resistance in specific types of deformed ice.

1.2. Objectives of the dissertation

The dissertation focuses on the study of sea ice deformation events in the Gulf of Finland and their impact on shipping. While ridges and other compressive deformed ice regions are hindrances to winter navigation, divergent elongated openings (leads) facilitate shipping.

The main objectives are to:

- analyze the processes and patterns of deformed (compressive) ice growth rate during severe winters with respect to realistic variable wind forcing (papers I and III);
- determine the long-term flaw lead occurrence frequency for the entire Gulf of Finland, including improved pattern estimates for the average duration of seasonal ice cover (paper II);
- analyze lead formation and compressive deformation patterns with respect to idealized wind forcing from different directions (papers II and III);
- study the relation of ship accidents to the dynamic ice conditions (papers I and III);
- estimate favorable segments for safe and economical wintertime shipping, where the probability of lead occurrence is highest and the probability of ridge formation is lowest (papers II and III).

For the analysis of sea ice deformation fields in the Gulf of Finland in the severe winter of 2002/03, the author performed a model simulation using the HELMI

(HELsinki Multicategory Ice) sea-ice model. The same model, with different forcing and options, is used also in the Finnish ice service. The analysis of modeled ice features was focused on two well-described events of ship damage. Further on, the author digitized the ice charts from the Estonian Meteorological and Hydrological Institute (EMHI) of the period 1971–2010 and analyzed spatial offshore patterns of flaw lead occurrence frequency in the context of the average duration of ice cover. In addition to the ice charts, the author used the MODIS satellite imagery to determine the leads distribution over the Gulf of Finland in winter 2002/03. In order to interpret the results, the author performed a series of numerical experiments with the HELMI model, using idealized wind forcing from different directions.

1.3. Basic concepts

Deformation is the main process that redistributes the ice mass over a waterbody. An obvious cause of ice deformation is its differential movement by winds and currents. Basic deformation processes are rafting, ridging and openings. When the wind impacts the ice floe to move and the ice motion is restricted, the ice cover starts to compact. After the floes are tightly compressed together, the **rafting** of ice begins, whereby one floe overrides or forms interlocking thrusts with another. This is followed by **ridging**, whereby the compression process results in the accumulation of an ice block both above and below the water surface. The subsurface part of the ridge yields the majority of its volume. Ridging and rafting are illustrated in Figure 3. Waterbodies with a specific shape and/or extent and a large variety of ice conditions are sensitive to rafting and ridging.

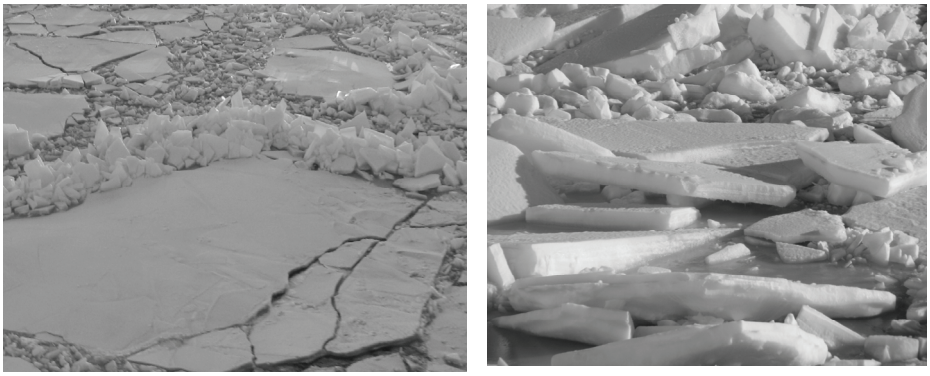

Figure 3. Typical ridging (left) and rafting (right) patterns of ice in the Gulf of Finland (*photos by the author*).

Deformed ice growth rate (dh/dt) is defined as the change of mean thickness h of ridged and rafted ice during unit time. In this paper the unit time is taken as 24 h. Together with rafting and ridging, open water areas form to the other side of the compression (Figure 4). Open water areas are defined as **leads**, which form between the areas of sea ice, for example, between pack ice and fast ice. The elongated leads enable winter navigation for vessels. A model experiment, used in the study, defines the leads as regions where the ice concentration is less than 85% and the ships can navigate without any difficulties. Low ice concentration grid points are equivalent to the lead areas.

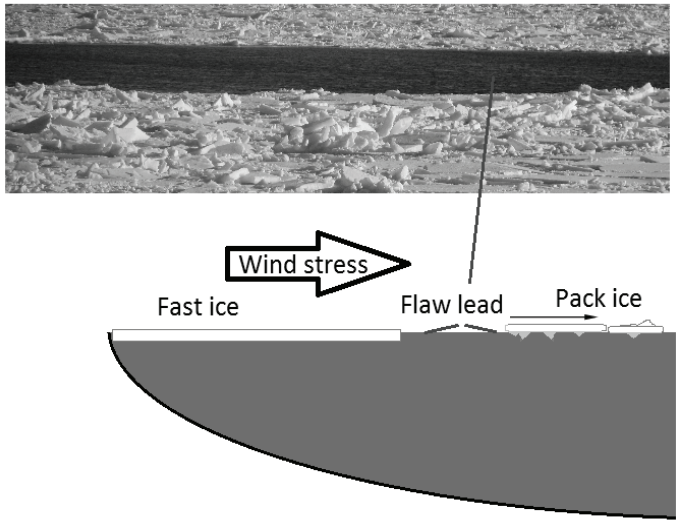

Figure 4. Photo (above) and conceptual scheme (below) of flaw lead formation. The width of flaw leads can be from tens of meters to tens of kilometers.

The time series of the climate characteristics indicate three winter types: the mild, the average and the severe. **Severe winter** according to the classification by Seinä and Palosuo (1996) begins from the maximum ice cover area of 279 000 km^2 (at least 75% of the sea area). For the Gulf of Finland, the prime object of the study, the whole gulf is already fully covered by ice when the Baltic-wide ice cover extends over 200 000 km^2 (*i.e.* during an average cold winter).

Sum of negative degree-days indicates the thermodynamic ice thickness growth and the extent of ice by summarizing negative degree-days under the melting point in a period.

2. THEORETICAL DESCRIPTION AND MODELING OF SEA ICE DYNAMICS

2.1. Basic approaches and equations

Sea ice is a complex material formed of water crystals, air and salt between them. Its physical properties are variable in space and time. Sea ice forms an ice cover, which is statically unstable in large basins and breaks into fields of ice floes forming drift ice. The nature of sea ice dynamics varies at a characteristic scale. The ice floe scale extends from 10 m to 10 km and includes individual floes and ice forms such as rubble, pressure ridges and fast ice. Drift ice or pack ice is of medium scale, and rheology and internal stress become relevant on high compact ice. Large scale sea ice models are determined mainly by external conditions, e.g. are used in global climate models. The following approach to ice dynamics is at the medium scale.

Sea ice is almost mobile (pack ice), except in coastal regions where ice grows out from and stays attached to the shore (fast ice). Pack ice is affected by several mechanical and thermodynamic processes. Mechanical processes result in the formation of leads and ridges as well as rafted ice. The total mass of sea ice remains in unchanged mechanical processes, but regionally sea ice thickness may vary drastically. The formation of leads results in the appearance of new areas of open water. The open water surface loses heat to the atmosphere thus starting new ice formation. Pack ice is a mixture of level ice, deformed ice and open water with great variability in thickness at a 10–100 m scale.

The life cycle of pack ice (Haapala, 2000) can be conceptually described by several steps:

1. Loosing heat to the air, the sea water surface cools to its freezing point creating a frazil ice layer;
2. Ice grows thermodynamically in thickness under continued cooling, maintaining its compactness during calm winds and forming floes of pack ice during stronger winds;
3. Pack ice is compressed and ice thickness grows there by mechanical deformation;
4. At compressing sites, pack ice is deforming (rafting and/or ridging); the ice rafts when a floe rides over another floe; when an ice floe is properly compressed or floes collide, ice pieces can break from a floe, and these ice pieces are able to agglomerate thus forming ridges;
5. Due to external mechanical factors (wind and/or current) ice floes move away from one another thus creating a lead, so the ice concentration falls there; when cooling continues, new ice will emerge in the lead;
6. Finally, when the air is warm again (above the freezing point), parts of the sea ice field melt at the rates that depend on their particular types.

Thermodynamic growth combined with divergent and convergent deformation forms a variable ice landscape. The thickness distribution function $g(h)$ characterizes the ice landscape formed in this way. Pack ice consists of a few different thickness classes. Each class has its own characteristic thickness distribution, also mechanical and thermodynamic properties. Some observed data are available to calculate $g(h)$ (Wadhams, 1998); however only a few numerical models are able to resolve it, and some trouble emerges here from the redistribution function Ψ (how one ice class affects another, see equations 1 and 2). The models are sensitive with respect to several characteristic variables.

A few early ice dynamics models assumed that sea ice field behaves as a viscous fluid. Hibler (1979) elaborated a viscous-plastic rheology and developed a sea ice dynamics model which contributed to modeling close ice conditions more naturally than the previous models. In his classical model, he considered only two categories of sea ice: the thin ice, which he treated as open water, and the thick ice. Most of the numerical models developed for the Baltic Sea follow his one. Hibler (1980) and Flato and Hibler (1995) proposed that the thickness distribution function $g(h)$ be solved numerically for each ice category separately. The multi-category sea-ice models apply the redistribution functions to describe the average evolution of ice deformation. A time step of the model may comprise a few deformation events: compacting, rafting and/ or ridging. Different physical ice classes are distinguished, introducing ice thickness categories $h(h_1 \ldots h_n)$ and related compactness $A(A_1 \ldots A_n)$. The packing compactness of the ice field may lie anywhere between zero and one and it changes easily (Vihma and Haapala, 2009).

Several models considering ice redistribution were developed for operational purposes. Leppäranta (1981) distinguishes between undeformed (level) and deformed ice. He treats level-ice thickness, ridge density, ridge sail height and total ice concentration as prognostic variables. A few models developed for the Baltic Sea (Omstedt, 1994; Zhang and Leppäranta, 1995; Haapala and Leppäranta, 1996; Schrum, 1997) follow this pattern with some specific distinctions.

However, Leppäranta´s (1981) model does not provide different equations to estimate the concentrations of level and deformed ice. Also, in this model he assumes the ice to ridge only in the event its concentration achieves unity through the convergent movement. Haapala (2000) simplified the ice thickness redistribution model treating pack ice as composed of open water, two various types of undeformed ice and of rafted, rubble and ridged ice. Thus he gained the advantage of considering the various ice types as thermally and mechanically separated. This model is recognized for estimating real seasonal pack ice evolution. Deformed ice emerges gradually depending on the storm activity. Haapala (2005) developed his model further resolving some parameterization-based difficulties related to the difference between Rothrock (1975) and Hibler (1979).

The mass conservation law is divided into conservation equations for the evolution of the compactness and thickness for each ice category:

$$\partial A_i/\partial t = -\mathbf{u}\nabla\cdot A_i + \Psi_i^A + \Phi_i^A, \quad (1)$$

$$\partial h_i/\partial t = -\mathbf{u}\nabla\cdot h_i + \Psi_i^h + \Phi_i^h, \quad (2)$$

where A_i and h_i are the compactness (fraction of ice cover area per surface sea area) and mean (in terms of ice volume per unit area) thickness of particular ice category i, $\mathbf{u}$ is the vector of ice drift velocity, Φ_i are the thermodynamic growth or decay rates, and Ψ_i are the thickness redistribution functions due to mechanical deformations, describing open water changes, rafting and ridging. The redistribution functions Ψ_i are dependent on ice thickness, compactness and strain rates (Thorndike *et al.*, 1975).

Drift ice behaves non-linearly outside the coastal zone. Sea ice with thickness below 20 cm drifts easily due to the winds and the currents. The theoretical free drift speed (2% of the wind speed; Leppäranta, 2005) fits well for such ice. The 20–50 cm thick ice has moderate mobility. Such ice usually passes shorter distances, and it can stick to fast ice zones near islands and shoals, for example Gogland. If the ice has grown thicker than 50 cm, the wind may be not able to cope with the yield stress of the ice, and the Gulf of Finland ice cover can persist during the mid-winter for up to two months (Leppäranta and Wang, 2002).

Ice motion is determined by the momentum balance equation, in Cartesian coordinates it reads

$$m\left(d\mathbf{u}/dt + f\,\mathbf{k}\times\mathbf{u}\right) = A(\boldsymbol{\tau}_a + \boldsymbol{\tau}_w) - mg\nabla\xi + \nabla\cdot\boldsymbol{\sigma}, \quad (3)$$

where m is the total ice and snow mass per unit area, $\mathbf{u}$ is the horizontal ice velocity vector, f is the Coriolis parameter, $\mathbf{k}$ is the upward unit vector, A is the mean (over different categories) ice concentration, $\boldsymbol{\tau}_a$ and $\boldsymbol{\tau}_w$ are the air (wind) and water stress vectors, $\nabla\xi$ is the sea surface gradient acting under gravity g and $\boldsymbol{\sigma}$ is the internal stress tensor. The internal ice stress $\nabla\cdot\boldsymbol{\sigma}$ depends on the strain rate, ice thickness h_i and ice compactness A_i of the ice field. For the ice compactness A_i below 0.8, we may also neglect the internal stress term. This approach is known as the free-drift concept (Leppäranta, 1994).

The winds are treated as an external force. The air stress transferred from atmosphere to the ice is

$$\boldsymbol{\tau}^a = \rho_a C_{ai}|\mathbf{u}_a|\mathbf{u}_a \ , \quad (4)$$

where ρ_a is the air density, C_{ai} is the air–ice drag coefficient and $\mathbf{u}_a$ is the wind velocity.

The dynamics of ice and water are coupled. The water–ice stress exerting at the ice bottom can be presented as (Leppäranta, 1981):

$$\boldsymbol{\tau}^{w} = \rho_w C_{wi} |\mathbf{u}_w - \mathbf{u}| [\mathbf{u}_w - \mathbf{u}], \tag{5}$$

where ρ_w is the water density, C_{wi} is the water–ice drag coefficient and $\mathbf{u}_w$ is the water current velocity. Leppäranta and Omstedt (1990) found 3.5×10^{-3} as a representative value for C_{wi} in the Baltic Sea.

2.2. Modeling of sea ice dynamics with HELMI sea ice model

Modeling the Baltic Sea ice dynamics began in the early 1970s with works by Udin and Ullersting (1976) and Leppäranta (1977). They assumed that an ice field behaves as a viscous fluid. Operational modeling began in winter of 1976/77 and was published by Leppäranta (1981), who presented a complete version of this model.

Based on the Hibler (1979) model with viscous-plastic rheology, Leppäranta and Zhang (1992) developed a similar model for the Baltic Sea. In their approach sea ice is a non-linear plastic continuum characterized by non-linear bulk and shear viscosities and the pressure term.

Haapala (2005) developed the HELMI model (HELsinki Multicategory Ice model). It resolves ice thickness distribution, i.e. ice concentrations of different thickness categories, redistribution of ice categories due to deformations, thermodynamics of sea-ice, horizontal components of ice velocity and internal stress in an ice pack. An ice pack is a mixture of open water and level ice and deformed ice categories of variable thickness. Deformed ice is divided into the rafted ice and ridged ice classes. The model has been used in large-scale studies (Haapala *et al*., 2005) and operational applications. The model physics and numerics are the same both in operational and research simulations. The only differences are the horizontal resolution and the scheme of atmospheric forcing used.

The present set-up of the sea ice model predicts the evolution of five level ice and two deformed ice categories. Ice categories are time-stepped in the thickness space without any limits, except the thinnest category, which is not allowed to exceed 10 cm in thickness. The horizontal resolution of the model is 1 nautical mile (1.852 km).

The author used atmospheric forcing from the NCEP/NCAR reanalysis project (paper I).

3. ANALYSIS OF ICE DEFORMATION EVENTS IN SEVERE WINTERS

3.1. General weather and ice conditions in the Gulf of Finland

Ice conditions during a typical severe winter (1995/96) in the Gulf of Finland are depicted in Figure 5. During the maximum ice extent, ridged ice covers large offshore areas of the gulf and ice thickens towards the eastern part of the gulf. Ice is ridging more severely in the narrowest part of the gulf between 25°E and 25°30´E and in its widest part between 27°E and 28°E. Also noteworthy north – south differences in ice properties are evident. As strongest winds blew from NW, N and NE before February 22 (prior to the compilation of the ice chart given in Figure 5), the ice drifted southwards generating a lead about 10–20 km offshore from the northern Finnish coast. At the boundary of landfast ice, ridges were formed in the compressive region in the southern and eastern boundaries, respectively.

The author chose the severe winter 2002/03 as the main period of the studies. The period stands out with its diversity: the whole Gulf of Finland was covered for a long time with ice of high concentration, severe weather conditions generated much deformation, numerous ship incidents happened.

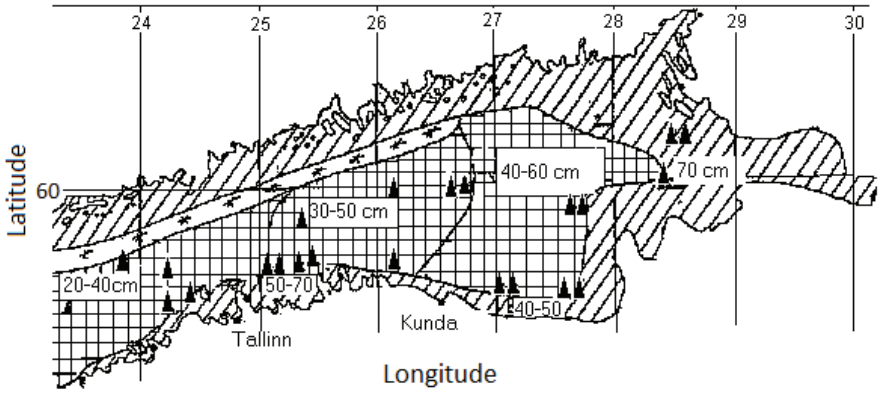

Figure 5. Ice chart on the date of the largest ice extent (February 22) in the ice season 1995/96. In previous few days winds blew alternately from N, NE and NW. The triangles denote ridged ice, diagonal lines fast ice and squares consolidated ice. The ice chart was provided by EMHI.

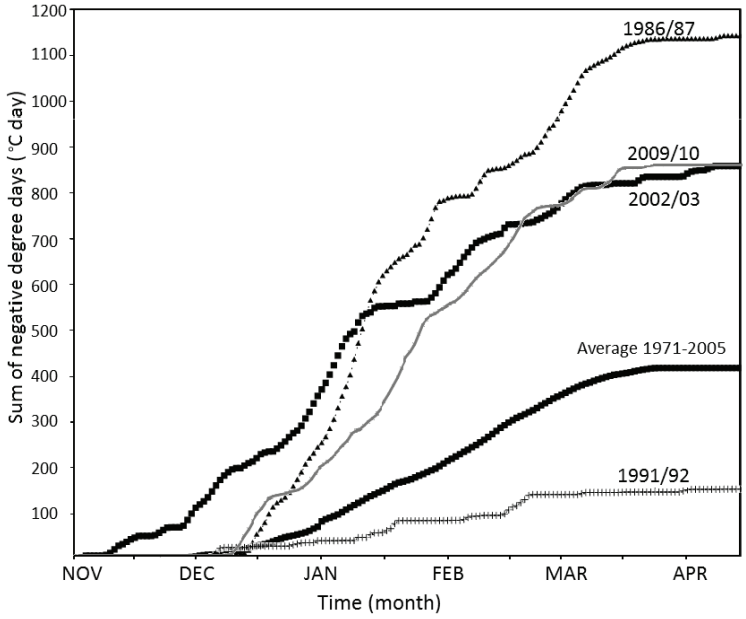

Figure 6. The sum of negative degree-days in the central Gulf of Finland. A very severe winter (1986/87), a mild winter (1991/92), a severe winter (2002/03), the last winter 2009/10 and the average for the winters of 1971/2005 are shown.

The winter season 2002/03 started very early and its beginning was the coldest over the last 40 years. In comparison with the average, the ice cover period lasted longer by one month. The number of cold degree-days increased faster than usually in late autumn 2002 (Figure 6). The cumulated sum in the average winter was 400°C and winter 2002/03 passed this number already at the beginning of January. The whole ice season was severer than in a mean winter, the sum of negative degree-days was over 800°C. The daily wind speed was above average in almost the whole season (Figure 7). The length of the sea lane that ships go through ice in the Gulf of Finland is usually about 100 km, but in the winter of 2002/03 it reached up to 400 km due to difficult navigation conditions. The ice-breaking period was then significantly longer than during an average winter. In 2003 the ice was very thick and deformed, navigation was difficult and navigational restrictions were valid for 117–149 days (Hänninen, 2003). Ice breaking is usually first needed in January, but during that winter ice breaking in the Gulf of Finland started already in December.

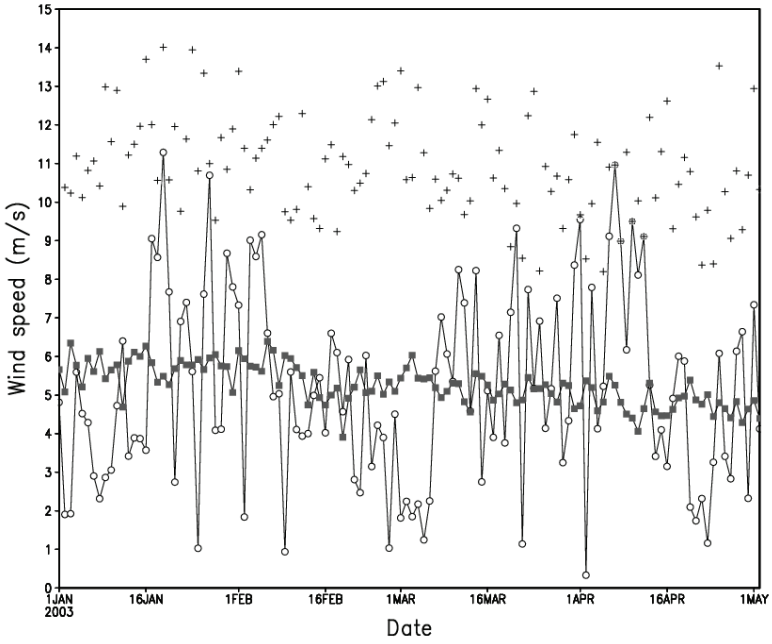

Figure 7. Daily wind speed from NCEP/NCAR reanalysis (the line with circles) for winter 2002/03, and mean (squares) and maximum (crosses) daily wind speeds during 1971–2005.

Ice extent is in correlation with the North Atlantic Oscillation (NAO) index values in severe and mild winters (Vihma and Haapala, 2009). When the NAO index is positive westerly airflow dominates, bringing mild weather into Northern Europe in winter. At the same time the ice extent in the Baltic Sea is not extensive. In case of a negative NAO index the westerly airflow is weak and winters are severe. Severe winter type is especially relevant for ship navigation in the Gulf of Finland. In mild winters SW winds dominate in the Gulf of Finland (Table 1), but in severe winters strong winds are blowing from N and NE. Winds from N and NW generate elongated leads favoring ship navigation (papers II and III).

Table 1. Percentage of winds from different directions on the Gulf of Finland (1971–2005 from the NCEP/NCAR reanalysis data (25.0 E, 60.0 N))

Direction	%
NE (0˚-89˚)	16
SE (90˚-179˚)	26
SW (180˚-269˚)	37
NW (270˚-359˚)	21

Average winter (January–March) air temperature at 2-m height is –2°C in the western part of the Gulf of Finland and up to –6°C in the eastern part when the NAO index is above 0.5. If the NAO index is below –0.5, then temperature is 2 degrees lower (Vihma and Haapala, 2009).

3.2. Deformed ice building and distribution

In a large restricted basin, like in the Gulf of Finland, sea-ice drift, caused by wind, has large horizontal gradients due to the vicinity of landlocked fast ice, causing sea-ice ridging in the compressive regions and opening of pack ice in the divergent regions.

We analyzed how ice deformation rates were related to wind speed and wind directions in the winter of 2002/03. As can be seen from Figure 8, wind speed alone does not determine the ice deformation rate but also wind direction is crucial in generating deformation. The wind modifies ice conditions essentially by raising stress in an ice field, resulting in compressive deformation of ice. Some ice fields can be significantly deformed even by a wind of 4 m/s if it blows from a suitable direction (III). Figure 8 shows that the E, S and NW winds tend to cause the most powerful deformation.

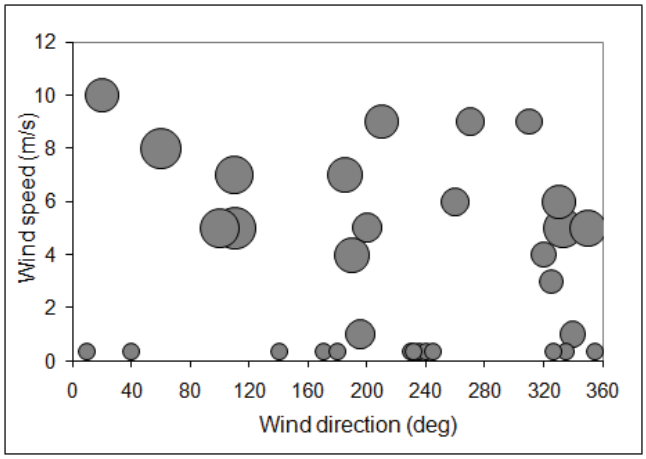

Figure 8. Growth rate of deformed ice related to wind direction and speed in winter 2002/03. The circles denote the average (over the Gulf of Finland) growth rate from 0.07 m/day to 0.18 m/day as shown by the circle diameter.

Model experiments performed to study the growth rate of deformed ice in the Gulf of Finland showed that the deformation of ice depended on the wind speed to some extent but was much more influenced by changes in the wind direction (Fig. 8).

For example, low winds (speed about 4 m/s) with variable direction were able to cause strong ice deformation, but stronger steady winds (about 9 m/s) could result in a lower deformation rate. In the Gulf of Finland the most intensive ridging generally took place when the wind blows from E, SW and NW.

A lead formation event of sea ice, appearing in one region, caused at the same time compressive deformations (ridging and thickening) in other regions. We analyzed also the cumulative deformation phenomena to characterize ridged and rafted ice distribution. To estimate the mean deformed ice thickness, the thickness was integrated over the latitudes 59.4N–60.5N. Figure 9 depicts how the mean deformed ice thickness varied in space and ice formed over time. According to the model calculations, more than 60% of the ice deformation events took place in the southern part of the Gulf of Finland. Also, the mass of deformed ice was greater in the southern part (Figure 9) and the deformation was twice as strong on the southern coast as on the northern coast. For example, at 60.2N, the average deformed ice thickness was 0.2 m, whereas at 59.5 N it was 0.5 m over the level ice.

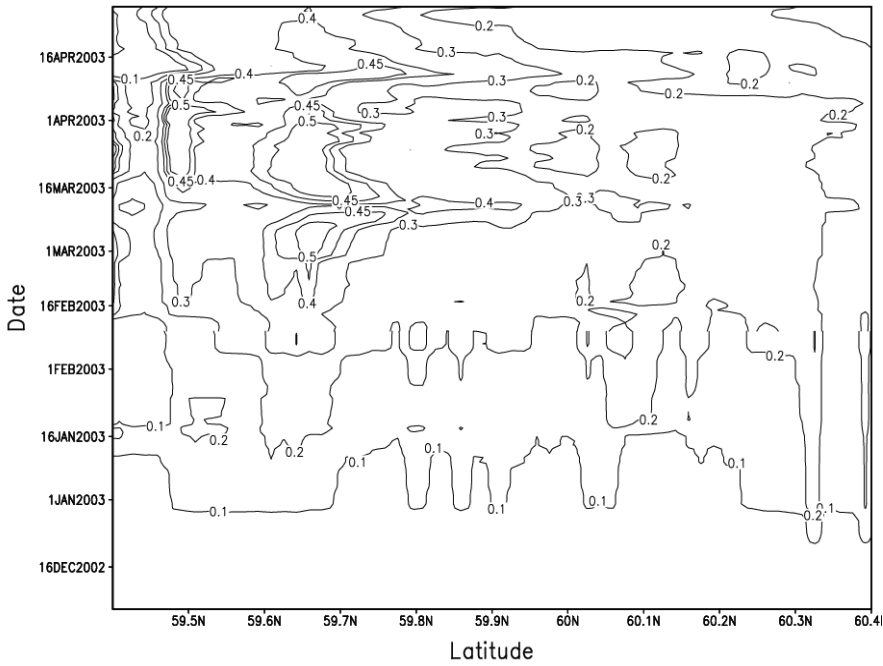

Figure 9. Growth of deformed ice thickness in various latitude sections. To characterize each section, the modeled deformed ice thickness was integrated over the latitude (along the parallels).

For an evaluation how important the mechanical thickening of ice is, we can make the following simple comparison of the deformed ice growth rates to the thermodynamic growth rate of ice. If the air temperature is –10°C, then 0.35 m

thick ice grows daily about 0.01 m. Thus the thermodynamic growth rate of the undeformed ice is small compared to that of deformed ice. In the same conditions, the new ice in the leads is thickening about 0.05 m a day.

Ridged ice areas were identified and analyzed as well. For every ice chart the area of deformation was identified on the basis of the symbols of ridged and rafted ice. The average number of ridging days in mild and severe winters in the northern and southern part of the Gulf of Finland is shown in Table 2. In mild winters, pack ice near the northern coast was deformed 1.5 times more frequently than on the southern coast. During severe winters it was vice versa: ridges occurred more frequently on the southern coast.

Table 2. The average of ridging days during 1971–2010

Winter type	Northern shore	Southern shore
Average	23	15
Severe	29	38

3.3. Ship hull damages and their relations to ice conditions

The relationship between the ship damage and deformed ice growth rate was examined. The basic data for the analysis were average ice deformation growth rates calculated by the HELMI ice model compared to ship damage events in the Gulf of Finland (paper I).

An ice deformation growth rate over 0.004 m/day occurred during 25% (28 days) of the winter season. In the examined period there were 49 ship damage events. The most of the damages (80%) took place in days when the average deformation rate exceeded 0.004 m/day. The deformation growth rates were the highest for the winter in the period 15–18.01.03, when the growth rate was up 0.018 m/day, and in the period 27–28.02.03, when the rate was up to 0.016. We note that in the first period eight accidents with the ship hull damaged by the ice took place in four days and in the second interval five accidents occurred in two days. In other periods ship damage events were not so frequent. Analysis indicates that the high ice deformation growth rate is related to the vessel damages in the Gulf of Finland.

We have selected two ship damage cases (Hänninen, 2003) from the winter 2002/03 to analyze. The ships were sailing along the leads or a ship channel and got stuck in compressive ice. We applied the HELMI model to identify compressive ice situations (paper I).

3.3.1. Ship damage case on January 11, 2003

A 95 000 DWT oil tanker, ice class IC, was on her way with cargo from Russia to Denmark when it got stuck in the compressive ice near Suursaar (27.5 E, 60.0 N) on January 11, 2003, and ice blocks piled up against the side of the ship (Hänninen, 2003).

The wind speed was only some 3 m/s in the morning of January 11 but in the evening it was up to 8 m/s. The wind direction gradually turned from N to SW during the day.

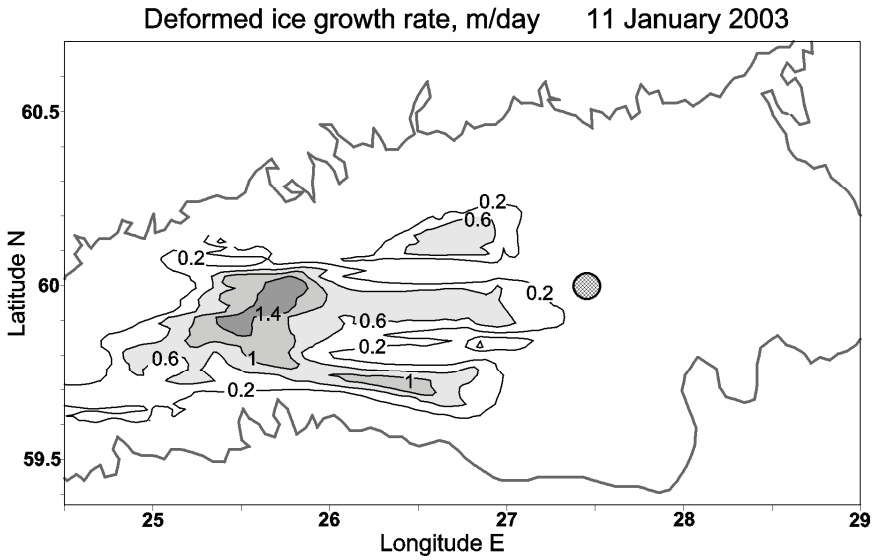

Figure 10. Simulated growth rate of deformed ice in the Gulf of Finland on January 11, 2003. The circle denotes the location where the ship damage occurred.

The damaged ship came from NE and incidentally entered into the compressive ice area. The exact time of the ship accident is not known to the author. According to observations, on the day before the ship accident the whole sea area was ice covered. The ice concentration was over 95% and the thickness of level ice ranged from 15 to 35 cm. The model simulations show a compression and production of new ridged ice around the place of damage during the time it occurred (Figure 10). The largest ridge production rates were modeled westward from the location of the accident, around longitudes 25.5–26.0 E. The daily growth rate of deformed ice was only 0.1 to 0.3 m/day in the region of the accident, but up to 1.4 m/day in the middle of the Gulf of Finland. This can be partly explained by the ice drift pattern (not shown) due to the changing wind conditions. The ice pack was nearly immobile around the ship damage location in the morning of January 11, but a fast SSE drift (more than 30 cm/s) was apparent westwards from the accident place. This situation caused large ridged

ice production in the middle of the Gulf of Finland and presumably high compressive forces around the accident place. By the evening of the day, the changed wind direction induced a nearly uniform northward drift with a speed of 10–12 cm/s all over the damage area. The average deformed ice growth rate over the entire Gulf of Finland was 0.008 m/day.

3.3.2. Ship damage case on January 21, 2003

A tugboat (240 DWT, ice class IA) was damaged in the Gulf of Finland on January 21, 2003, due to the moving and compressive ice field. The accident took place at the end of the lead, at the beginning of an ice field (about 60.15 N and 25.2 E). The ship stuck in the ice field and started to drift along the ice masses with a speed of 2–3 knots. Ice pieces piled up against the ship's side shell. The pile-up process and drifting lasted about 20 minutes, then the compression ceased and ice pieces started to slide below the ship bottom. The ship drove to the fast ice field and waited for the icebreaker assistance (Hänninen, 2003).

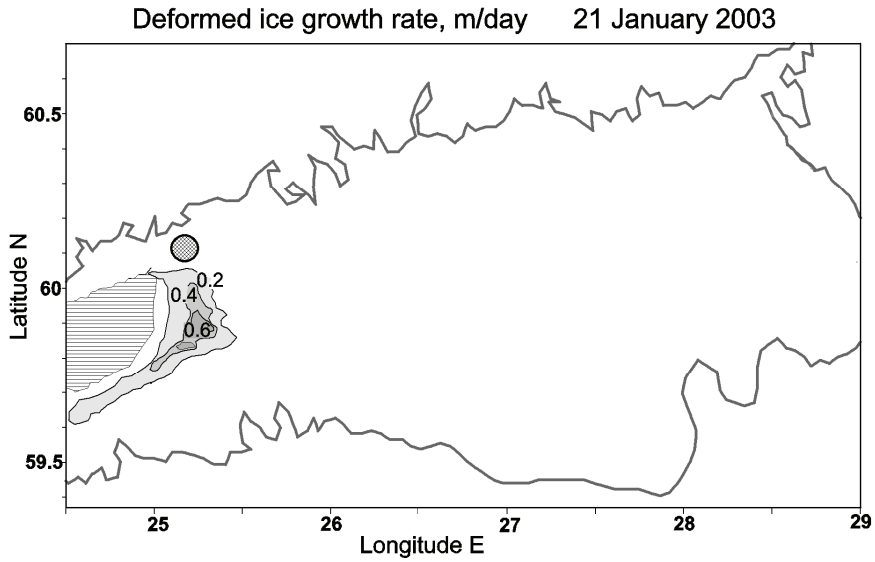

Figure 11. Simulated growth rate of deformed ice in the Gulf of Finland on January 21, 2003. The hatched area is free water with ice concentration less than 10%. The circle denotes the location where the ship damage occurred.

The wind speed fluctuated from 2 to 7 m/s on January 20–22. Higher speeds of up to 10 m/s were observed earlier on January 19. On January 20, a day before the accident, the wind turned from N to SW and then stayed in the southerly direction.

The observed ice thickness and concentration revealed large gradients in space on those days. An ice lead extended from the western entrance in the northern part of the Gulf of Finland, with the ice thickness below 10 cm and concentration below 20%. In the eastern part of the central Gulf of Finland, the level ice thickness increased above 30 cm and the ice concentration above 90%. In the area where the ship damage occurred, the total ice concentration was 70–99%. According to the model results, this area contained mostly deformed ice. The mean total ice thickness in the region was over 70 cm, whereas the mean ridged ice fraction was 60–80%. Modeling results (Figure 11) show that a strong deformation took place only in a small area to the south from the location of the ship damage, at the edge of the ice margin, ridging offshore (0.6 m/day). The northward drift of ice was the highest (14 cm/s) in the area with a low ice concentration.

At the northern border of the lead, the ice pack was almost motionless. This differential ice drift probably contributed to a high compressive stress in the ice pack. The state finds confirmation in the logbook observation. The average growth rate was 0.004 m/day over the entire sea, which is the lowest criterion for ship damage analysis. However, the above mentioned conditions made the local area very complicated.

4. IMPACT OF FLAW LEADS ON THE SHIPPING IN THE GULF OF FINLAND

4.1. Leads as natural fairways

Openings in ice are a common feature in the Gulf of Finland. An open water area can sometimes extend over several hundred kilometers. If a lead lies along the Gulf of Finland axis, it facilitates navigation through the area. In the Gulf of Finland the W, NW, N and S winds generate leads that are wide enough for a vessel to navigate through. This is particularly important with regard to severe winters when the Gulf of Finland is fully covered with thick and ridged ice. Previous studies have shown that during average winters, leads are more common in the Estonian coastal region (paper II). But during severe winters the northern winds blow more frequently and thus there are more flaw leads in the northern part of the gulf.

The question is how facile is the formation of elongated leads and do they facilitate shipping in the ice field? Further on, how steady are the leads?

4.2. Observed ice deformations

The dominating winds in the Gulf of Finland are from SW. A logical presumption could be that ice ridges occur mostly in the northern coast and wind generates openings in the south. The following observational analysis reveals the opposite. The modeling study (paper II) described in the previous chapter shows that SW winds create a few irregular unconnected open water areas which do not facilitate shipping in ice when the Gulf of Finland is ice covered. Due to the shape of the gulf the NW winds, which represent 21% of all the winds, produce the most navigable leads or openings elongated along the direction of the gulf's axis. The N and S winds also create conditions for the formation of leads facilitating shipping through the Gulf of Finland. The S and SE winds create leads near the southern coast.

To investigate the occurrence of leads facilitating shipping we studied MODIS satellite images from the year 2003 (Figure 13, paper III). Analysis contained altogether 51 images and the results are given in Table 3. In total, 14 irregular openings were identified. Most of the leads (in 22 cases) emerged near the Finnish coast and only two leads near the Estonian coast.

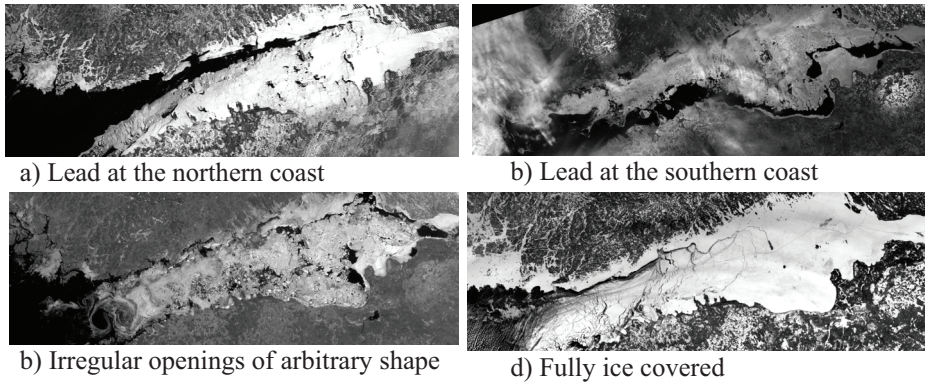

a) Lead at the northern coast

b) Lead at the southern coast

b) Irregular openings of arbitrary shape

d) Fully ice covered

Figure 13. Ice situation in the Gulf of Finland in 2003. Moderate Resolution Imaging Spectrometer images (MODIS).

Table 3. Occurrence of natural leads in the Gulf of Finland in the winter of 2003 from MODIS images

Ice condition	Frequency
Elongated leads near the Finnish coast	22 times
Elongated leads near the Estonian coast	2 times
Fully ice covered	13 times
Irregular openings of arbitrary shape	14 times

The occurrence of leads in different regions of the Gulf of Finland was also observed according to the EMHI ice charts in the period 1971–2010. In the analysis, the lead was defined as a narrow linear region of open water, new ice or a region of low ice concentration located either between two areas of compact ice or between pack ice and fast ice. Severe winters and the average of all winters are observed.

The statistics for the ice cover period and occurrence of leads (percentage of the ice days) in different regions of the Gulf of Finland was calculated for the regular 1.0° × 0.2° grid in longitude and latitude, respectively. We also examined which areas are favorable for navigation and harbors, assuming a low ice concentration allow leads to favor shipping, whereas the regions of high ice concentration are typically regions of deformed ice, which build obstacles to navigation.

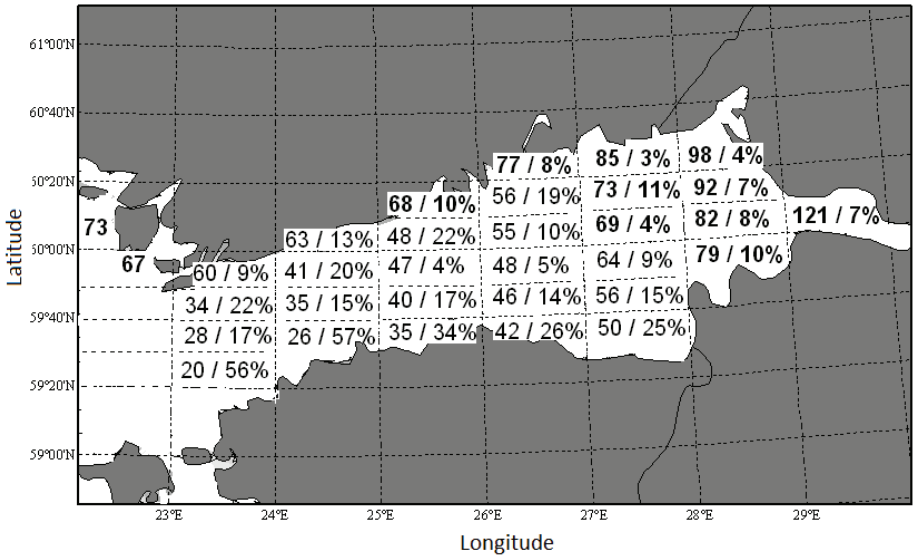

Figure 14. Average ice conditions in the Gulf of Finland during 1971–2010 in the 1.0° × 0.2° grid. The numbers in cells show the average duration of ice cover in days and the percentage of ice lead occurrence of the ice cover duration (% of the ice days).

The average of all winters shows that leads occur most often in the Estonian coastal area, where their occurrence is typically 10 – 30% (Figure 14). In the middle of the Gulf of Finland leads make up a much smaller percentage. For example, between 25°E and 26°E, leads accounted only for 4% in the middle of the basin, whereas the occurrence increased to 22% at the Finnish coast and to 34% at the Estonian coast. The lead fraction was highest in the entrance of the Gulf of Finland. The reason is a thin ice cover due to the short ice-cover period, which makes the ice cover very mobile under the action of winds and ocean currents.

In order to find the relation between the wind direction and the spatial pattern of lead occurrence, the wind distribution was calculated for the days when the daily wind speed exceeded 4 m/s as lower wind speeds are not expected to cause ice drift.

In the following section we analyze historical ice cover data in the Gulf of Finland during severe winters when the ice cover extended over 200 000 km^2 in the Baltic. These winters, relying on the historical ice charts, were in 1979, 1980, 1982, 1985, 1986, 1987, 1994, 1996, 2003, 2006 and 2010.

In severe winters when the Gulf of Finland is fully ice covered the duration of the ice season becomes more uniform all over the Gulf of Finland. In a severe winter the SW winds dominate but the NW and N winds are also present.

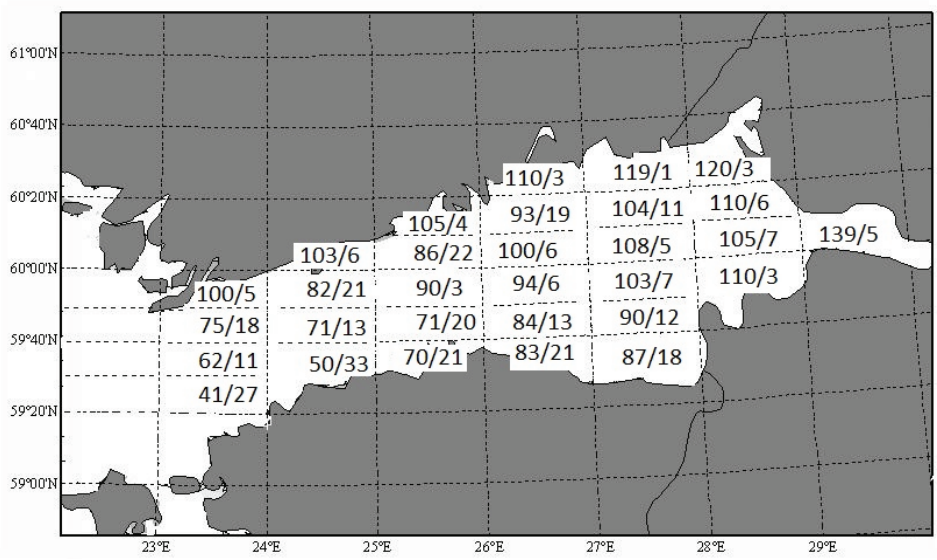

Fig 15. Average ice conditions in the 1.0° longitude × 0.2° latitude grid in the Gulf of Finland in severe winters during 1971–2010. The first number in the cell is the average duration of ice cover in days and the second one is the occurrence of leads in days.

A statistical overview of lead occurrence in severe winters is given in Figure 15, with the average duration of ice cover days and the occurrence of leads in days. Subtracting the occurrence of leads from the duration of ice cover we find how many hindrance days there were. We can notice that leads occur in the middle of the basin less often than in its northern part. Besides, more ice days are characteristic of the middle part. The average ice cover duration is calculated considering the ice break-up in springtime. If the lead formation lasted longer than a week, the days after that were considered ice-free days. In severe winters wind-created leads occur mostly near the Finnish coast. The results indicate differences in lead formation for the average and severe winter.

4.3. Results from numerical experiments

The objective was to find out which winds generate elongated leads, using the experiments with the HELMI model. We estimated the relationship of wind direction to open water formation and ice deformation rate.

The results are based on idealized numerical experiments, where sea ice was initially constant: the level ice thickness was set 0.35 m, the ice concentration A = 0.99. Then the response of the sea-ice model for different wind directions with constant wind speed of 10 m/s was calculated. In order to analyze which wind directions facilitate navigation in ice, we assumed that in those regions where the modeled ice concentration was less than 85%, the ships could navigate without any difficulties. Low ice concentration grid points were regarded as lead areas.

When a northerly wind was acting, an extensive flaw lead, parallel to the coast line, extended from the mouth to the end of the Gulf of Finland (Figure 12 N and Figure 5). In that case, vessels could easily navigate in the Finnish coastal zone. However, the picture was quite different when a north-easterly wind was blowing. This wind situation generated also much open water, but contrary to the previous case, open water areas were separated by an island, and a uniform lead was generated only in the easternmost part of the Gulf of Finland (Figure 12 NE and Figure 13 b).

Also southerly winds, blowing transverse to the basin, were favorable for lead generation (Figure 12 S). In this case the lead was located at the Estonian coast reaching from the mouth (23°E) up to the central part of the Gulf of Finland (28°E), while a few minor leads did exist by the Ingerian (southern) shore of the Gulf of Finland (between 28°E and 29°E). Examination of the MODIS satellite images and EMHI ice charts for all winters of 1971–2010 reveals that the model results fit well with the observational data.

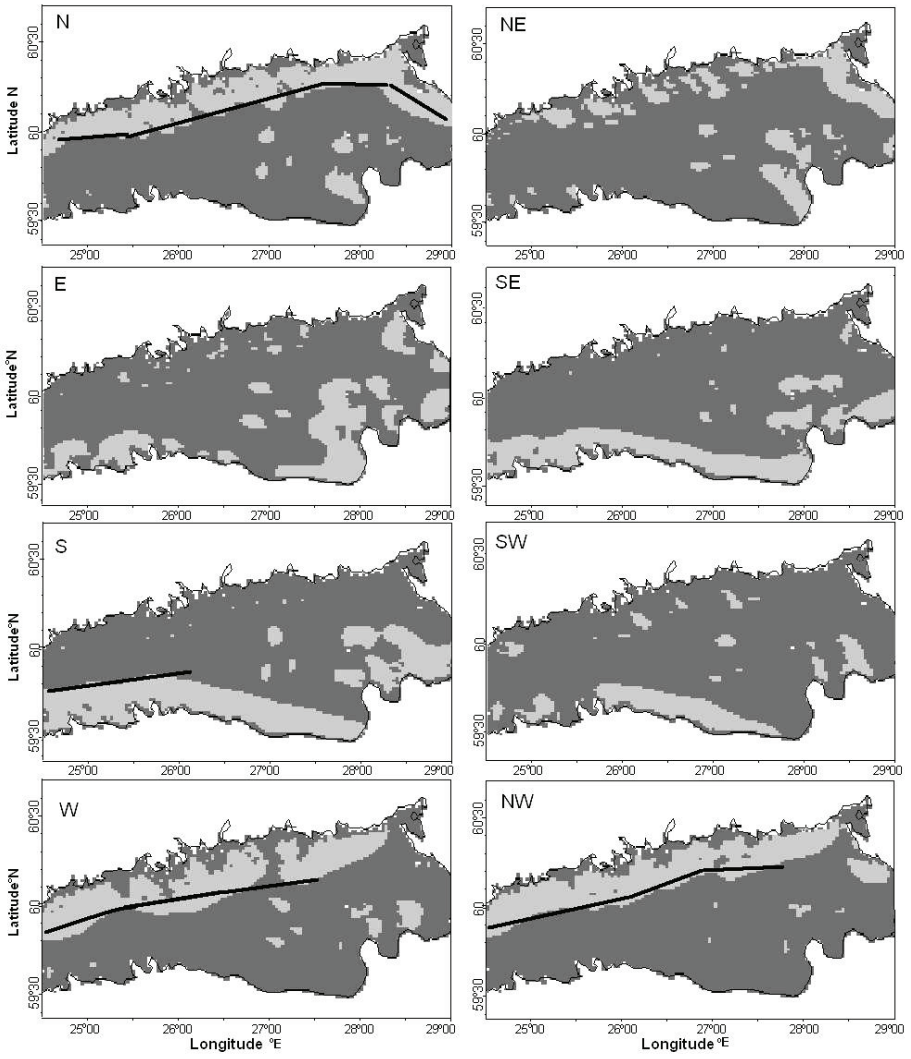

Figure 12. Ice conditions favoring vessel navigation along the Gulf of Finland when a constant wind acts at least 10 h. W, NW, N and S winds generate a rather uniform lead pattern and thus facilitate navigation in the ice.

5. DISCUSSION AND CONCLUDING REMARKS

Which areas would be reasonable for shipping routes in the Gulf of Finland in severe winters considering the main navigation along the gulf in the west and east directions?

If we take into account only the ice conditions the best area for ship navigation is the northern part of the gulf. Here most of the natural elongated leads and open water suitable for shipping occur. In the winter of 2002/03 elongated leads appeared near the northern coast at least on 22 days. The southern part is an alternative considering the appearance of leads. The number of average ice days is lower in the southern part compared to the northern part. Suitable elongated leads appear as well, but less frequently. On the other hand, a lot of ridged ice, more harmful for shipping than level ice, lies near the southern coast. Compressive ice, which is the greatest hindrance to the shipping activity, can be found in the central line of the Gulf of Finland where the official fairways are located. Elongated leads practically do not appear in this area.

However, the ice conditions are not the only factors in planning shipping fairways. The sea is shallower on the northern side of the gulf and there are many dangerous shoals. One more aspect to be reckoned with in ship route design is the probability of coastal oil pollution from accidental spills.

In the following summary of the dissertation, the main findings of the studies on which it is based are presented.

- The deformed ice growth rate in the Gulf of Finland depends on the wind speed to some extent but it is much more influenced by the wind direction. Most intensive ridging generally takes place when the wind blows from E, SW and NW.
- About 60% of the ice deformation events took place in the southern part of the Gulf of Finland during 1971–2010. Also according to the model results over 60% of the deformed ice mass was generated in the southern part in the severe winter of 2002/03.
- The two ship damages in winter 2002/03 happened close to the high growth rate area of deformed ice at the interface of different ice conditions with notable ice thickness gradients. It is concluded that the rate of ridged ice production is an indicator of the compression of the ice pack. Probably even larger compressive forces had occurred in the locations of ship damages.
- In the mild winters during 1971–2010, pack ice near the northern coast was deformed 1.5 times more frequently than at the southern coast. During the severe winters ridges occurred 1.3 times more frequently at the southern coast.
- The high ice deformation growth rate is related to the vessel damages in the Gulf of Finland. During the winter season of 2002/03 there were 49 ship damages in the Gulf of Finland. About 80% of the ship damages took

place on days when the average deformed ice growth rate was over 0.004 m/day. In about 25% of the days during this period the ice deformation growth rate was between 0.004 and 0.027 m/day.

- Elongated leads are particularly important in severe winters when the Gulf of Finland is fully ice covered. Winds from W, NW, N and S generate uniform leads that are wide enough for vessels to navigate through the ice.
- During the average winters in 1971–2010, leads were more common in the southern coastal region. During the severe winters northern winds blew more frequently and leads appeared in the northern part of the Gulf of Finland. According to the MODIS (Moderate Resolution Imaging Spectrometer) images elongated leads appeared near the northern coast 11 times more often than in the southern coast in the winter season of 2002/03.
- The dominating SW winds create a few irregular unconnected open water areas which do not facilitate shipping in ice when the Gulf of Finland is ice covered. NW winds, which represent 21% of all the winds, produce the best navigable leads or openings elongated along the direction of the gulf's axis.
- In the middle of the Gulf of Finland leads made up the smallest percentage: leads formed only on 4% of all the ice days. The occurrence increased to 22% at the northern coast and to 34% at the southern coast.

REFERENCES

Dethleff, D., Loewe, P. & Kleine, E. 1998. The Laptev Sea flaw lead – detailed investigation on ice formation and export during 1991/1992 winter season. *Cold Reg. Sci. Technol.*, 27, 225–243.

Flato, G.M. & Hibler III, W.D. 1995. Ridging and strength in modeling the thickness distribution of Arctic sea ice. *J. Geophys. Res*., 100, 18611–18626.

Haapala, J. 2000. Modelling of the seasonal ice cover of the Baltic Sea (Ph. D thesis). Report series in Geophysics, 42. University of Helsinki, Dept. of Geophysics. 41 pp.

Haapala, J. & Leppäranta, M. 1996. Simulating the Baltic Sea ice season with a coupled ice-ocean model. *Tellus A*, 48 (5), 622–43.

Haapala, J. & Leppäranta, M. 1997. The Baltic Sea ice season in changing climate. *Boreal Environ. Res*., 2 (1), 93–108.

Haapala, J., Lönnroth, N. & Stössel, A. 2005. A numerical study of open water formation in sea ice. *J. Geophys. Res.*, 110, C09011.1–C09011.17.

Haas, C. 2004. Airborne EM sea-ice thickness profiling over brackish Baltic Sea water. In: *17th International Symposium on Ice*, pp. 12–17. International Association of Hydraulic Engineering and Research, Saint Petersburg.

Hänninen, S. 2003. Incidents and accidents in winter navigation in the Baltic Sea, winter 2002–2003. Finnish Maritime Administration Research Report, 54. Helsinki. 39 pp.

HELCOM. 2006. Report on shipping accidents in the Baltic Sea area for the year 2006. 27 pp. http://www.helcom.fi/stc/files/shipping/

HELCOM. 2007. Towards a Baltic Sea with environmentally friendly maritime activities. In: *2nd Stakeholder Conference on the HELCOM Baltic Sea Action Plan*. Helsinki, 2007.

Hibler III, W.D. 1980. Modeling a variable thickness sea ice cover. *Monthly Weather Rev.,* 108, 1943–1973.

Hibler, W. D. 1979. A dynamic thermodynamic sea ice model. *J. Phys. Oceanogr*., 9, 815–846.

Jaagus, J. 2006. Trends in sea ice conditions on the Baltic Sea near the Estonian coast during the period 1949/50–2003/04 and their relationships to large-scale atmospheric circulation. *Boreal Environ. Res.*, 11, 169–183.

Jevrejeva, S., Drabkin, V.V., Kostjukov, J., Lebedev, A.A., Leppäranta, M., Mironov, Ye.U., Schmelzer, N. & Sztobryn, M. 2004. Baltic Sea ice seasons in the twentieth century. *Climate Res*., 25, 217–227. 53.

Kotovirta, V., Jalonen, R., Axell, L., Riska, K. & Berglund, R. 2009. A system for route optimization in ice-covered waters. *Cold Reg. Sci. Technol.*, 55, 52–62.

Kujala, P., Hänninen, M. & Ylitalo, J. 2009. Analysis of the marine traffic safety in the Gulf of Finland. *Reliab. Eng. Syst. Safe*., 94 (8), 1349–1357.

Langhorne, P. (ed.) 2002. *Proc. 16th IAHR Ice Symp.*, Vol. 2, pp. 353–357. University of Otago, Dunedin, New Zealand.

Lensu, M. 2003. The evolution of ridged ice fields. Helsinki University of Technology, Report M-280. Espoo. 140 pp.
Leppäranta, M. 1981a. An ice drift model for the Baltic Sea. *Tellus*, 33 (6), 583–596.
Leppäranta, M. 1981b. On the structure and mechanics of pack ice in the Bothnian Bay. *Finn. Mar. Res.*, 248, 3–86.
Leppäranta, M. 2005. *The Drift of Sea Ice.* Springer-Praxis, Heidelberg.
Leppäranta, M. & Hakala, R. 1992. Structure and strength of first-year sea ice ridges in the Baltic Sea. *Cold Reg. Sci. Technol*., 20, 295–311.
Leppäranta, M. & Myrberg, K. 2009. *Physical Oceanography of the Baltic Sea*. Springer-Praxis, Heidelberg. 378 pp.
Leppäranta, M. & Wang, K. 2002. Sea ice dynamics in the Baltic Sea basins. In: *Proc. 16th IAHR Ice Symposium*, Vol. 2, pp. 353–357. Dunedin, New Zealand.
Leppäranta, M. & Zhang, Z. 1992. A viscous-plastic ice dynamic test model for the Baltic Sea. Finnish Inst. of Marine Res., Internal Report 3.
Leppäranta, M., Tikkanen, M. & Shemeikka, P. 1998. Observations of ice and its sediments on the Baltic coast. *Nord. Hydrol*., 29 (3), 199–220.
Liu, C., Chang, Y.-C., Huang, S., Yan, S.-Y., Wu, F., Wu, A.-M., Kato, S. & Yamaguchi, Y. 2009. Monitoring the dynamics of ice shelf margins in Polar regions with high-spatial- and high-temporal-resolution space-borne optical imagery. *Cold Reg. Sci. Technol.*, 55, 14–22.
Omstedt, A. 1990. A coupled one-dimensional sea ice–ocean model applied to a semi-enclosed basin. *Tellus*, 42A, 568–582.
Omstedt, A., Nyberg, L. & Leppäranta, M. 1994. *A Coupled Ice–Ocean Model Supporting Winter Navigation in the Baltic Sea, Part 1. Ice Dynamics and Water Levels*. Reports Oceanography, 17. SMHI, Norrköping. 17 pp.
Palosuo, E. 1975. Formation and structure of ice ridges in the Baltic. Winter Navigation Research Board, Rep. No. 12. Helsinki.
Rothrock, D.A. 1975. The energetics of the plastic deformation of pack ice by ridging. *J. Geophys. Res*., 80 (33), 4514–4519.
Schrum, C. 1997. An ice/ocean model for North and Baltic Sea. In: *Sensitivity of the North Sea, Baltic Sea and Black Sea to Anthropogenic and Climatic Changes*. NATO Advanced Science Inst. Series, Vol. 27, pp. 311–325.
Seinä, A. & Palosuo, E. 1996. The classification of the maximum annual extent of ice cover in the Baltic Sea 1720–1995. *Meri*, 27, 79–91.
Seinä, A. & Peltola, J. 1991. Duration of the ice season and statistics of fast ice thickness along the Finnish coast 1961–1990. *Finn. Mar. Res*., 258. 46 pp.
Siegel, H., Gerth, M. & Tschersich, G. 2006. Sea surface temperature development of the Baltic Sea in the period 1990–2004. *Oceanologia*, 48 (S), 19–131.
Similä, M., Karvonen, J., Haas, C. & Hallikainen, M. 2006. C-Band SAR based estimation of Baltic Sea ice thickness distributions. In *Proc. IEEE*

International Geoscience and Remote Sensing Symposium, IGARSS 2006. Denver.

Sonninen, S., Nuutinen, M. & Rosqvist, T. 2006. Development process of the Gulf of Finland Mandatory Ship Reporting System. *VTT Publ.* Espoo, pp. 12–30.

Soomere, T., Myrberg, K., Leppäranta, M. & Nekrasov, A. 2008. The progress in knowledge of physical oceanography of the Gulf of Finland: a review for 1997–2007. *Oceanologia*, 50, 287–362.

Stein, R. & Korolev, S. 1994. Shelf-to-basin sediment transport in the eastern Arctic Ocean. In: H. Kassen et al. (eds.), *Russian–German cooperation in the Siberian shelf seas: Geo-system Laptev-Sea. Ber. Polarforsch.*, 44, 87–100.

Swedish Meteorological and Hydrological Institute. 1982. *Climatological Ice Atlas for the Baltic Sea, Kattegat, Skagerrak and Lake Vänern (1963–1979)* Printed by Söfartsverkets tryckeri, Norrköping.

Tarand, A. N. & Nordli, P.Ø. 2001. The Tallinn temperature series reconstructed back half a millennium by use of proxy data. *Climatic Change*, 48, 189–199.

Thorndike, A.S., Rothrock, D.A., Maykut, G.A. & R. Colony, R. 1975. The thickness distribution of sea ice. *J. Geophys. Res*., 80, 4501–4513.

Udin, 1. & Ullerstig, A. 1976. A numerical model for forecasting the ice motion in the Bay and Sea of Bothnia. Res. Rep. No. 18. Winter Navigation Research Board, Norrkoping, Sweden.

Vihma, T. & Haapala, J. 2009. Geophysics of sea ice in the Baltic Sea – a review. *Progr. Oceanogr*., 80, 129–148.

Wadhams, P. 1998. Sea ice morphology. In: M. Leppäranta (ed.), *Physics of Ice-Covered Seas*, pp.231–288. Helsinki University Press, Helsinki.

Zakharov, V.F. 1966. The role of flaw leads off the edge of fast ice in the hydrological and ice regime of the Laptev Sea. *Acad. Sci. USSR*, 6, 815–821.

Zhang, Z. & Leppäranta, M. 1995. Modeling the influence of ice on sea level variations in the Baltic Sea. *Geophysica*, 31 (2), 31–45.

ABSTRACT

The Gulf of Finland is one of the most intensive ship traffic areas in the world. In severe and average winters the mean ice cover lasts for 140 days. Sea ice represents a great danger and hindrance for ships. Sea ice conditions are very variable and dynamic. In certain conditions openings in ice and elongated leads form, which favor ship navigation and decrease the risk of accidents. Flaw leads and ice ridges are common features in the Gulf of Finland.

The Gulf of Finland is one of the hazardous regions of the Baltic Sea. In winter 2002/03 almost 60% of all ship hull damages of the Baltic Sea took place in this gulf. Over 50 incidents happened at the Finnish coast in winter 2010, whereby the ship was stuck in ice for several hours or days

The study uses the numerical sea ice model to determine conditions forming leads of favorable shape and relations between ridged ice and ship damages. The occurrence frequency of leads and ridges in different regions of the coast in the past 35 years is analyzed.

The results of the analysis show firstly that the two ship accidents treated took place at the interface of different ice types, where ridge ice thickness grew remarkably. This allows speculations that the number of ship accidents could be reduced by introducing ice model forecasts into the navigation support. Secondly, considering ice conditions, the best suitable area for ship navigation along the coast is the northern side, where leads favorable to ship navigation are formed most often. Leads occur on average 3–6 days per winter along the central axis, 11–23 days near the northern coast and 6–19 days at the southern coast. At the southern coast the occurrence of ridged ice is approximately twice as frequent as near the northern coast, which could hinder shipping near the southern part. The most favorable winds generating leads along the coast are NW-N, NE-E and S winds.

RESÜMEE

Soome laht kattub jääga külmadel ja keskmistel talvedel. Tekkinud merejää, mille kestus on kuni 140 päeva, on talvisel meresõidul peamiseks takistuseks ja ohuks laevadele. Tuuled põhjustavad jää ümberpaiknemist, tekivad vabavee avaused ja lahvandused, mis on sage nähtus Soome lahel. Teatud tingimustel kujunevad pikad ja piklikud lahvandused, mis võiks soodustada laevaliiklust. Teisalt tekivad pinged jääkattes, moodustades laevadele ohtlike rüsi- ja ladejää moodustisi, mille paksus ulatub 15 m-ni. Soome laht on Läänemere ohurikkamaid piirkondi, kus 2002-2003 aasta talvel toimus ligikaudu 60% laevakere vigastustest. Talvel 2010 oli Soome lahel üle 50 juhtumi, kus laev takerdus mitmeks tunniks või päevaks jäässe.

Autori eesmärgid olid:

- Uurida rüsi- ja ladejää mõju laevakere kahjustustele Soome lahes talvel 2002-2003 (III)
- Rakendada numbrilist jäämudelit, et välja selgitada deformeerunud jääpaksuse kasvu kiiruse seos kahe laevavigastusega talvel 2002-2003 (I) ja laevadele soodsate lahvanduste tekkimise looduslikud tingimused (II).
- Analüüsida lahvanduste esinemise sagedust lahe eri piirkondades viimase 35 aasta jooksul (III).

Tulemustest selgus:

- Deformeerunud jää kasvumäär sõltub tuule kiirusest teatud määral, kuid on rohkem mõjutatud tuule suunast. Kõige intensiivsemalt jää deformeerub E, SW ja NW tuulte mõjul.
- Töös on analüüsitud numbrilise jäämudeli (HELMI) väljundandmeid,. Mõlemad avariid juhtusid erinevate jääliikide üleminekualal, kus esines märkimisväärne deformeerunud jääpaksuse kasv.
- Külmadel talvedel (vahemikus 1971-2010) esines ligikaudu 60% jää deformatsiooni juhtumitest lahe lõunapoolses osas. Sama kinnitavad ka mudelarvutused, mille kohaselt moodustus külmal talvel 2002/2003 60% deformeerunud jää massist lahe lõunapoolses osas.
- Võrreldes Soome lahe põhja- ja lõunapoolseid alasid, selgub, et pehmetel ja keskmistel talvedel on rüsi ja ladejää sagedus 1,5 korda suurem mere põhjapoolsel alal. Külmadel talvedel on aga rüsi- ja ladejää sagedus 1,3 korda suurem lõunapoolsel alal.
- Deformeerunud jää kasvu määr on seotud laevakahjustustega Soome lahel. Talvel 2002/2003 oli Soome lahel 49 laevakere kahjustust. 80% õnnetustest toimus päeval, kui keskmine deformeerunud jää kasvutempo oli üle 0,004 m ööpäevas. Vastav kasvukiirus oli talvel 2002-2003 25% päevadest.

- Keskmisel talvel (vahemikus 1971-2010) esinevad lahvandused peamiselt Soome lahe lõunapoolses osas. Külmadel talvedel seevastu on lahvanduste esinemissagedus suurem põhjapoolses osas. Satelliidi (MODIS) pilte järgi oli talvel 2002-2003 navigatsiooniks sobilikke lahvandusi põhjarannikul 11 võrra rohkem kui lõunakaldal.
- Lahvandused pikki Soome lahte on eriti olulised külmadel talvedel, kui laht on jääga täielikult kaetud. Soodsaimad tuuled, mis genereerivad navigatsiooniks soodsaid lahvandusi pikki Soome lahte, on NW- N, NE-E ja S tuuled. Soome lahel domineerivad SW tuuled põhjustavad ebaregulaarseid ja mitteseotud jäävabasid alasid, mis ei soodusta laevaliiklust.
- Talvine laevaliiklus piki Soome lahte kulgeb peamiselt lahe kesktsoonis. Uuringutulemused näitavad, et see on kõige ebasoodsam piirkond, kuna selles piirkonnas on lahvanduste sagedus keskmiselt 3-6 päeva talve jooksul. Soodsaim on liigelda Soome lahe põhja kalda poolses alas, sest seal on suurim lahvanduste sagedus, 11-23 päeva talve jooksul. Lõunakaldal aga 6-19 päeva, kuid lõunakaldal esineb ligilähedaselt kaks korda sagedamini rüsijääd.

ACKNOWLEDGEMENTS

First, with deep gratitude and pleasure, I would like to thank my supervisors Prof. Jüri Elken and Dr. Jari Haapala for guiding me through my doctoral studies. Also I would like to thank the Finnish Institute of Marine Research (FIMR/FMI), what enabled me conditions to work productively. The main concept of my dissertation originates from that time and matured further.

I also thank ice field promoter Prof. Matti Leppäranta, who has contributed my ice researching knowledge and experience. My colleagues from Marine Optical group leaded by Helgi Arst (Ants Erm, Aina Leeben, Anu Reinart and Liis Sipelgas), whom which we have together done a lot of fieldworks and held discussions about science.

I would like to express my gratitude to Tiia Kaare, Jevgeni Rjazin for editing the manuscript in English.

I greatly appreciate the support received from my friend Sigre and wish to express thanks to my sons Uku and Ott, whom with we have had fun on the ice and "icebergs" to conquer.

CURRICULUM VITAE

1. Personal data

Name	Ove Pärn
Date and place of birth	May 9, 1971, Paide

2. Contact information

Address	Akadeemia tee 15a, 12618 Tallinn, Estonia
E-mail	ove@sea.ee

3. Education

Educational institution	Graduation year	Education (field of study/degree)
Tallinn University, Institute of Mathematics and Natural Sciences	2001	Physics/ MSc
Tallinn University, Institute of Mathematics and Natural Sciences	1999	Physics/ BSc

4. Language competence/skills (fluent; average, basic skills)

Language	Level
Estonian	Native language
English	average
Russian	average

5. Special Courses

Period	Educational or other organization
1995-96	Music therapy specialist (Tallinn University)

1994-95	Health education (Tallinn University)
October 12–19, 2003	Advanced Study School: Nonlinear Processes in Marine Sciences (TUT)
May 11–16, 2009	Summer School on Physical Oceanography of the Baltic Sea (University of Helsinki)

6. Professional Employment

Period	Organization	Position
2007 – to date	Tallinn University of Technology , Institute of Marine Systems	Researcher
2002 – 2007	Tallinn University of Technology , Institute of Marine Systems	Engineer
1999 – 2002	University of Tartu, Faculty of Science and Technology, Estonian Marine Institute	Engineer

7. Publications (last 5 years)

Articles indexed by the ISI WEB of Science (1.1):

1. Pärn, O., Haapala, J. 2011. Occurrence of synoptic flaw leads of sea ice in the Gulf of Finland. Boreal Environment Research, 16, 71–78.
2. Leia, R., Leppäranta, M., Erm, A., Jaatinen, E., Pärn, O. 2011. Field investigations of apparent optical properties of ice cover in Finnish and Estonian lakes in winter 2009. Estonian Journal of Earth Sciences, 60, 50–64.

Pre-reviewed articles in other international research journals (1.2):

3. Pärn, O., Haapala, J., Kõuts, T., Elken, J., Riska, K. 2007. On the relationship between sea ice deformation and ship damages in the Gulf of Finland in winter 2003. Proceedings of the Estonian Academy of Sciences. Engineering, 13, 201–214.

4. Reinart, A., Pärn, O. 2006. Ice conditions of a large shallow lake (Lake Peipsi) determined by observations, an ice model, and satellite images. Proceedings of the Estonian Academy of Sciences. Biology, Ecology, 55, 243–261.

Articles in proceeding indexed by the ISI WEB of Science (3.1):

5. Pärn, O., Haapala, J. & Sipelgas, L., 2010. Leads as natural fairways in the Gulf of Finland, Baltic International Symposium (BALTIC), 2010 IEEE/OES US/EU, 1– 7, doi: 10.1109/BALTIC.2010.5621638

Articles in proceedings:

6. Jaatinen, E., Leppäranta, M., Erm, A., Ruibo, L., Pärn, O., Arvola, L., Kiiltomäki, A. 2010. Light conditions and ice cover structure in Lake Vanajavesi. In: Proceedings of the IAHR Symposia, 1–8.
7. Pärn, O., Haapala, J., Rjazin, J. 2009. Generation of coastal lead in Gulf of Finland. In: Matti Leppäranta (Ed.). Proceedings of the Sixth Workshop on Baltic Sea Ice Climate . Helsinki: University of Helsinki, 56–70.
8. Jaani, A., Klaus, I., Pärn, O., Raudsepp, U., Zadonskaja, O., Gronskaja, T., Solntsev, V. 2008. Hüdroloogia. In: Haberman, Juta; Timm, Tarmo; Raukas, Anto (Eds.). Peipsi. Tartu: Eesti Loodusfoto, 113–155.
9. Pärn, O., Haapala, J. 2007. Analysis of the Ice Model Simulation for the Gulf of Finland in 2002/2003. In: Fifth Workshop on Baltic Sea Ice Climate: Baltic Sea Ice Climate Workshop 2005. Schrum, Corinna; Schmelzer, Natalja (Eds.). Hamburg und Rostock, Germany: Bundesamt für Seeschifffahrt und Hydrographie, 2007, (BSH Bericht), 23–31.
10. Pärn, O. 2006. Jäänähtuste ja veetemperatuuri tundlikkus kliima muutusele. In: Tartu Ülikooli ilmade observatooriumi 140. juubeli konverentsi ettekanded: Kaasik, Marko and Post, Piia (Eds.) Tartu Ülikooli Kirjastus, 97–106.
11. Pärn, O. 2006. Jäämudeli analüüs, talvise meresõidu riskid. Kaasaegse ökoloogia probleemid: loodushoiu majandushoovad : Eesti X Ökoloogiakonverentsi lühiartiklid : Tartu, 27.-28. aprill, 2006. Tartu: Eesti Ökoloogiakogu, 2006, 173–177.

10. Other research projects

1. (ETF) Application of an operational oceanographic model system to study the Baltic Sea large- and mesoscale circulation patterns
2. (EU) Development and pre-operational validation of upgraded GMES Marine Core Services and capabilities (MyOcean)
3. (EU) SAFEWIN - Safety of Winter Navigation in Dynamic Ice

Paper I

Pärn, O., Haapala, J., Kõuts T., Elken J. & Riska, K. 2007. On the relationship between sea ice deformation and ship damages in the Gulf of Finland in winter 2003. *Proc. Estonian Acad. Sci. Eng*., 13, 201–214.

Proc. Estonian Acad. Sci. Eng., 2007, **13**, 3, 201–214

On the relationship between sea ice deformation and ship damages in the Gulf of Finland in winter 2003

Ove Pärn[a], Jari Haapala[b], Tarmo Kõuts[a], Jüri Elken[a] and Kaj Riska[c]

[a] Marine Systems Institute, Tallinn University of Technology, Akadeemia tee 21, 12618 Tallinn, Estonia; ove@sea.ee
[b] Finnish Institute of Marine Research, Erik Palménin aukio 1, FIN-00560 Helsinki, Finland; jari.haapala@fimr.fi
[c] ILS Oy, Lauttasaarentie 48 C, FIN-00200 Helsinki, Finland; kaj.riska@ils.fi

Received 24 April 2007, in revised form 26 June 2007

Abstract. Sea ice ridges and other types of deformed ice are the main obstacles for the winter navigation. During the severe winter 2002/2003, about 60% of the ship hull damages, registered in the Baltic Sea, occurred in the Gulf of Finland. We have analysed ice deformation features, derived from the HELMI sea ice model in relation to two ship damages that occurred in the Gulf of Finland this winter. The damages happened close to the high growth rate area of deformed ice at the interface of different ice conditions with notable ice thickness gradients. It is concluded that the rate of ridged ice production is an indicator of the compression of the ice pack and a potential indicator of ice-induced danger to shipping.

Key words: Gulf of Finland, sea ice, winter navigation, ice deformation, ship damage.

1. INTRODUCTION

The Gulf of Finland is an elongated (in the W–E direction) sub-basin of the Baltic Sea with the total length of 460 km and the width up to 120 km (Fig. 1). It is an important corridor for merchant and passenger shipping for its coastal states Estonia, Finland and Russia. More than 37 000 ships over 300 GRT cross (enter or leave) the entrance line of the Gulf of Finland annually, based on the data from the Automatic Identification System (AIS) for monitoring the maritime traffic in the Baltic Sea area [1,2]. The shipping intensity has an increasing trend due to the strong economic growth in this region, including tanker traffic to the new Russian oil terminals [2,3]. And the number of tanker accidents seems to increase

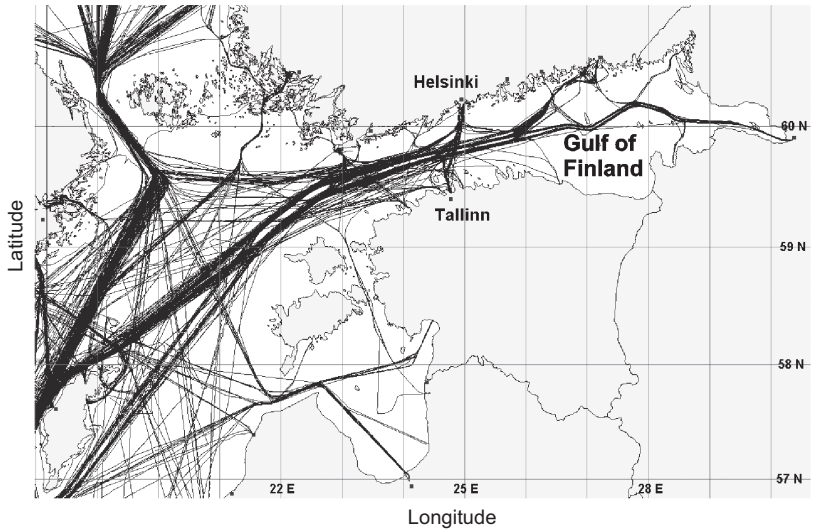

Fig. 1. Map of the Gulf of Finland in the northeastern Baltic Sea. Selected ship routes from the first half of April 2007 are shown by the HIROMB-SeaTrackWeb data (Swedish Meteorological and Hydrological Institute; the routes not necessarily represent the long-term shipping statistics).

when the winter is more severe. In the Baltic Sea shipping regulations, special attention is paid to the most dangerous wintertime navigation period [4,5] when vessels navigate through the ice.

The Gulf of Finland is fully ice-covered in normal and severe winters [6,7]. Even in very mild winters some parts of the Gulf of Finland freeze. Sea ice conditions substantially vary in the east–west direction. The average length of the ice season exceeds 120 days in the eastern part and is only a couple of weeks in the western entrance area of the gulf. The sea ice formation begins first in the eastern part of the Gulf of Finland, usually in the beginning of December. The break-up of ice cover occurs commonly in the middle of April, but in the coastal zone and small bays the land-fast ice may persist even until the beginning of May. The thickness of undeformed level ice is typically 30–40 cm but may reach 80 cm in certain snow-free conditions.

The most significant obstacles for the winter navigation in the Baltic Sea are pressure ridges and brash ice. They are particular forms of deformed (compressed) ice that develops under variable wind stress. Outside the land-fast ice region (depths down to 5–15 m) [8], the deformation of the pack ice is a key process determining the evolution of the distribution of the sea ice thickness. The dominant deformation processes are pressure ridging (piling of smaller ice blocks broken from interacting ice sheets) and rafting (overriding of one ice sheet by another). Recent ice thickness measurements in the Baltic Sea [9] have shown

that the amount of deformed ice is significantly larger than reported in the routine ice charts. Consequently, the mean ice thickness could exceed 1–2 m in large areas of the Baltic Sea. Sea ice ridges are the thickest ice forms. The visible part of the ridge, called sail, is typically 1–3 m high while the most of the ridge volume is contained in the subsurface part of the ridge, the depth of which may reach up to about 25 m in the Baltic Sea [10,11].

Modelling of the Baltic Sea ice dynamics started more than twenty years ago [12]. It has provided valuable results both in research and in operational applications. Among a number of ice model variables, observational validation and detailed analysis are usually done for the ice thickness and concentration, for different types of ice [13,14]. The progress in simulating the above "standard output" variables and ice drift velocity has increased the interest in the deformation-related model variables like the ridge height, the fraction of deformed ice and the rate of ice compression.

High pressure in the ice field causes ice deformation and can be dangerous to the vessels. In a severe winter 2002/2003, about 62% of ship hull damages, registered over the entire Baltic Sea, occurred in the Gulf of Finland, whereas 30% of damages were caused by ship–ice interaction and 15% of hull damages occurred in the ice field under compression [15].

In the present paper we perform an analysis of sea ice deformation fields in the Gulf of Finland in relation to ship damage events in winter 2003, based on the results from the HELMI sea ice model that is used also in the Finnish ice service. The analysis is a step towards the determination of actual ice loads on ships in operational situations, contributing to a better management of winter navigation. A brief presentation of the sea ice model used is given first, followed by a description of observed and modelled ice conditions in the particular winter. Finally, we focus on the analysis of modelled ice features during two events of ship damage.

2. DESCRIPTION OF THE HELMI MODEL

The HELMI (HELsinki Multicategory Ice (model)) model describes the spatial and temporal evolution of sea ice thickness distribution. It tracks ice concentrations of different thickness categories, the redistribution of ice categories due to deformations, the horizontal components of ice velocity and the internal stress of the ice pack and accounts for the thermodynamics of sea ice. The physics of the model with some applications to the climate studies is described in detail in [16,17]. In the Baltic Sea, the HELMI model has been applied for the regional sea ice forecasting (http://polarview.fimr.fi). The only differences between the operational and climate applications are in the horizontal resolution and in the scheme of atmospheric forcing.

The equations for the ice concentration and thickness for each ice category read

$$\partial A_i/\partial t = -\mathbf{u}\cdot\nabla A_i + \Psi_i^A + \Phi_i^A, \tag{1}$$

$$\partial h_i/\partial t = -\mathbf{u}\cdot\nabla h_i + \Psi_i^h + \Phi_i^h, \tag{2}$$

where A_i and h_i are the concentrations of the ice cover area per sea surface area and the mean (in terms of the ice volume per unit area) thickness of the ice category i, $\mathbf{u}$ is the vector of ice drift velocity, Φ_i are the thermodynamical growth or decay rates and Ψ_i are the thickness redistribution functions due to mechanical deformations, describing open water changes, rafting and ridging.

The redistribution functions Ψ_i depend on the ice thickness, concentration and strain rates [18,19]. Continuum scale sea ice models resolve an average behaviour of the pack ice and the subgrid scale processes are either neglected or taken into account in a simplified manner. Presently the HELMI model approximates the complex nature of sea ice forms by seven thickness categories. For the undeformed ice (level ice), we use five categories. The first undeformed ice category is typically the oldest and thickest ice due to the thermodynamical growth. The fifth undeformed ice category describes the growth of new ice in the leads. The deformed ice is separated into two ice thickness categories, one for rafted ice and the other one for the ridged ice. Ice categories are not bounded by the minimum and maximum ice thickness, except the thinnest category that is not allowed to exceed 10 cm in thickness.

The following assumptions are made regarding the deformation processes: 1) the deformed ice is generated only from undeformed ice categories, 2) the cross-over thickness determines whether the undeformed ice is rafted or ridged. These assumptions are based on the Parmeter law [20] and field observations [21]. It is also assumed that the thinnest 15% of the ice categories experience deformation [18]. Further assumptions are that the shear deformations are not taken into account and the shape and porosity of the ridges are constant. These assumptions are based on the results of field observations [10,22].

Ice motion is determined by the momentum balance equation

$$m(\mathrm{d}\mathbf{u}/\mathrm{d}t + f\,\mathbf{k}\times\mathbf{u}) = A(\boldsymbol{\tau}_a + \boldsymbol{\tau}_w) - mg\nabla\xi + \nabla\cdot\boldsymbol{\sigma}, \tag{3}$$

where m is the total ice and snow mass per unit area, $\mathbf{u}$ is the horizontal ice velocity vector, f is the Coriolis parameter, $\mathbf{k}$ is the upward unit vector, A is the overall mean ice concentration, $\boldsymbol{\tau}_a$ and $\boldsymbol{\tau}_w$ are the air (wind) and water stress vectors, $\nabla\xi$ is the sea surface tilt, g is the acceleration due to gravity and $\boldsymbol{\sigma}$ is the internal stress tensor. The internal stress of pack ice is calculated according to the viscous-plastic rheology [23]. This formulation also relates the consumption of kinetic energy to the ice pack deformations [24].

The HELMI sea ice model employs curvilinear coordinates. The variables are spatially discretized on the Arakawa C-grid. The advective part of the ice thickness and the concentration equations are solved by an upwind method. The momentum balance equation is solved by the line successive relaxation procedure, proposed by Zhang and Hibler [25].

In the present study we use the horizontal grid step of 1 nautical mile (1852 m). The model domain covers the whole Baltic Sea. The results are mainly analysed for the Gulf of Finland, but for comparison purposes also for the Gulf of Riga. For atmospheric forcing we used the data from the NCEP/NCAR reanalysis project (http://dss.ucar.edu/pub/reanalysis/).

3. OBSERVED AND MODELLED ICE CONDITIONS IN THE GULF OF FINLAND DURING WINTER 2002/2003

The air temperature time series given in Fig. 2 show that the cold season 2002/2003 began rather early. The temperatures were below the long-term average during most of the November and in December. Also the first half of January was relatively cold. The end of January was warmer than the average. February was again colder than the average. The entire winter 2002/2003 was the coldest over the last 34 years.

The Baltic Sea ice season 2002/2003 started already in early November with rapid ice formation in the northern Bothnian Bay, in the eastern part of the Gulf of Finland and in the coastal areas of the Gulf of Riga. By the end of December the entire Gulf of Finland was ice-covered. The ice thickness ranged from 15 cm in its western part to 50 cm in the eastern area [26]. Already in January vessels had to navigate through the ice along the longest way in 40 years. The icebound sailing distance reached up to 200 nautical miles instead of average 50 nautical miles.

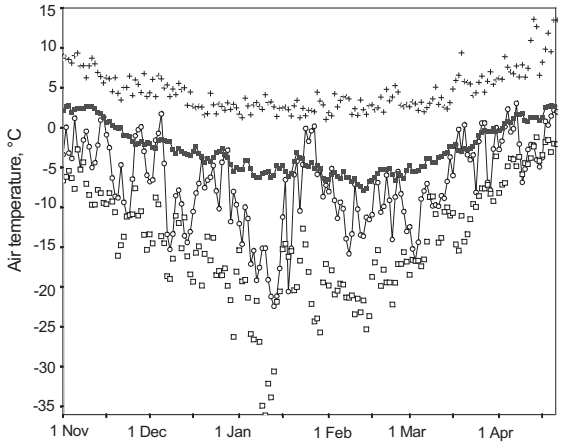

Fig. 2. Daily averages of the air temperature (circles) in the Gulf of Finland during winter 2002/2003. Filled squares show the average air temperature for the period of 1971–2005; unfilled squares and crosses represent the daily minimal and maximal air temperature for 1971–2005 from the NCEP/NCAR reanalysis data, respectively.

A specific feature of the winter 2002/2003 was the exceptionally thick ice. The level ice thickness was up to 80 cm on the Finnish coast. The ice thickness in the drift ice was even larger. According to the airborne electromagnetic measurements the mean ice thickness exceeded 1.5 m in several areas in late February [27]. Navigational conditions in the northern regions of the Baltic Sea were difficult and restrictions were valid 117–149 days during the whole winter. Typically, merchant ships need ice breaker assistance in the Gulf of Finland beginning with January; however during the winter season 2002/2003 icebreakers were needed already beginning with December. The maximum ice extent for the whole Baltic Sea was observed on March 5, when the ice-covered area was up to 232 000 km^2 [7]. According to this, the winter 2002/2003 is classified as an average ice winter [6], but certainly ice conditions in the Gulf of Finland were harder than on the average [7]. The length of the Gulf of Finland ice season in winter 2002/2003 exceeded the long-term average by more than a month.

The evolution of ice conditions during the entire winter was studied applying the HELMI model in the hindcast mode. Already in the beginning of January the total ice extent reached the maximum for a normal winter and the mean ice concentration was more than 90% over the Gulf of Finland area (Fig. 3). During the first half of January, the ice concentration decreased remarkably due to wind-induced deformation processes. From the mid-January the mean ice concentration decreased from 95 to 70% in the Gulf of Finland. The concentration is compared with the neighbouring Gulf of Riga with similar atmospheric conditions: 1) initial ice extent growth was delayed by about two weeks, 2) in the second half of January the mean ice concentration was reduced more drastically – from about 90 to 20–40%, 3) in February the concentration increased to about 60%, but remained

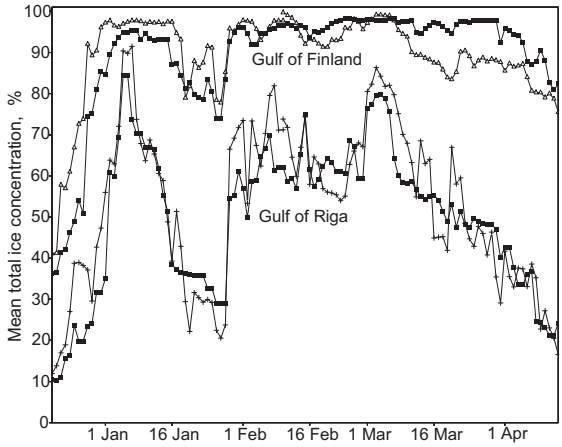

Fig. 3. Modelled (crosses and triangles) and observed (filled squares) mean total ice concentration (all ice categories) over the gulfs of Finland and Riga during winter 2002/2003.

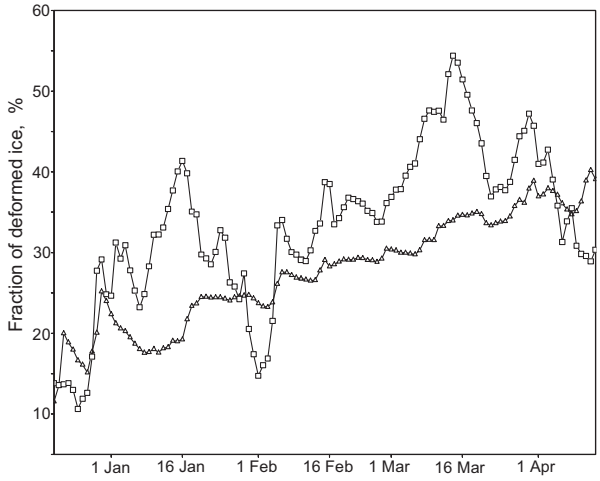

Fig. 4. Modelled time series of the average deformed ice fraction as part of the total ice concentration in the Gulf of Finland (triangles) and the Gulf of Riga (squares) during winter 2002/2003.

until the break-up by more than 30% lower than in the Gulf of Finland. The simulated mean ice concentrations in both of the gulfs are in a good agreement with the observed values.

The portion of deformed ice in total ice thickness is a good measure of the significance of the deformation process in the total ice balance. The time series of the fraction of deformed ice over the whole Gulf of Finland and the Gulf of Riga were calculated from the model outputs. The results of this calculation (Fig. 4) show that the bulk intensity of deformation processes is higher in the Gulf of Riga. Generally, the fraction of deformed ice increases from 15–20% of the whole ice cover in the beginning of winter up to 30–35% before the break-up. The highest fractions of deformed ice were up to 35% in the Gulf of Finland and up to 55% in the Gulf of Riga.

4. CASE STUDY OF ICE COMPRESSION EVENTS IN THE GULF OF FINLAND

In the ice-covered sea, most of merchant ships are able to proceed only along the artificial ice channels and natural leads and openings. An artificial ice channel is broken by an icebreaker or another powerful ship. An ice channel in the open sea is not in a stable state since it is exposed to external (mainly to wind) forcing. If wind is strong enough to bring the ice fields into motion, a compression in the ice cover frequently occurs. In some cases, the ice pack remains stationary although strong winds are acting. Horizontal differences in the field of ice motions cause

compression and compacting (an increase of the ice concentration), but also decompression (a decrease of the concentration or even formation of openings) in the ice cover. Navigation in compressive ice is very difficult and sets special demands to ships.

We have performed two case studies to analyse the situations where ships were sailing along the leads or a ship channel and stuck in compressive ice. Compressive ice situations were identified with the use of the daily growth rate of deformed ice categories (that is, changes owing to rafting and ridging) extracted from the HELMI model.

Model experiments, performed earlier to study the deformed ice growth rate in the Gulf of Finland, showed that the deformation of ice depends on the wind speed to some extent but is much more influenced by changes in the wind direction. For example, low winds (speed about 4 m/s) with variable direction are able to cause strong ice deformation, but stronger steady winds (about 9 m/s) may result in a lower deformation rate. In the Gulf of Finland the most intensive ridging generally takes place when wind blows from SW, SE or NW [28].

4.1. Ship damage on January 11, 2003

Wind conditions in January are given in Fig. 5 as measured at the Tallinn Harbour. Wind speed was only 3 m/s in the morning of January 11, but in the evening reached 8 m/s. The wind direction gradually turned from N to SW during the day.

A 95 000 DWT Oil tanker, ice class IC with cargo was on her way from Russia to Denmark when she got stuck in the compressive ice near Suursaar (27.5°E, 60.0°N) on January 11, 2003, and ice blocks piled up at side shells of the ship [15].

The damaged ship came from NE and incidentally entered into the compressive ice area. The exact time of the ship accident is not known to the authors. According to the observations, on the day before the ship accident the whole sea area was ice covered. The ice concentration was over 95% and the thickness of level ice ranged from 15 to 35 cm. The model simulations show a compression and production of the new ridged ice around the damage place during the time of the accident (Fig. 6). The largest ridge production rates (up to 1.4 m/day in the middle of the Gulf of Finland) were modelled westward from the location of the accident, around longitudes 25.5–26.0°E. The daily growth rate of deformed ice (that is the increase of the mean thickness of ridged and rafted ice during a 24 h period) was only from 0.1 to 0.3 m/day in the region of the accident. The occurrence of compression areas can be partly explained by the ice drift pattern (not shown) due to changing wind conditions. The ice pack was nearly immobile around the ship damage location in the morning of 11 January, but a fast SSE drift (more than 30 cm/s) was apparent westwards from the accident place. This situation caused intense ridged ice production in the middle of the Gulf of Finland and presumable high compressive forces around the accident place. By the evening of the day, changed wind direction (Fig. 5) induced a nearly uniform northward drift with a speed of 10–12 cm/s all over the damage area.

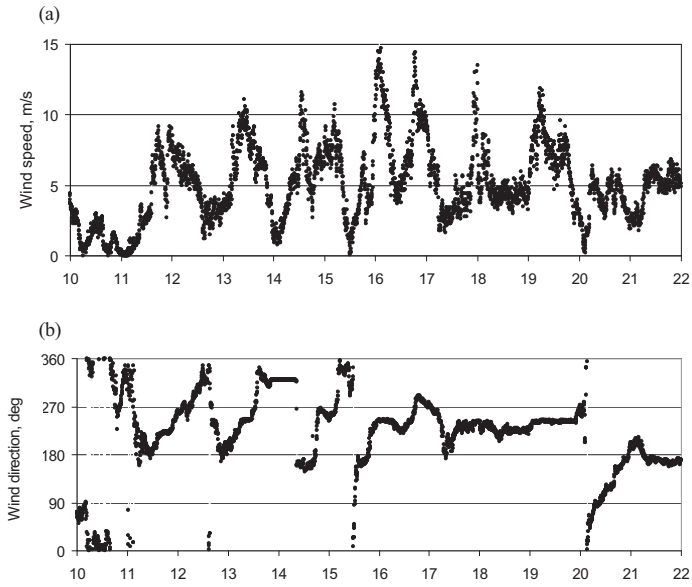

Fig. 5. Wind speed (a) and direction (b), measured at Tallinn Harbour during January 2003.

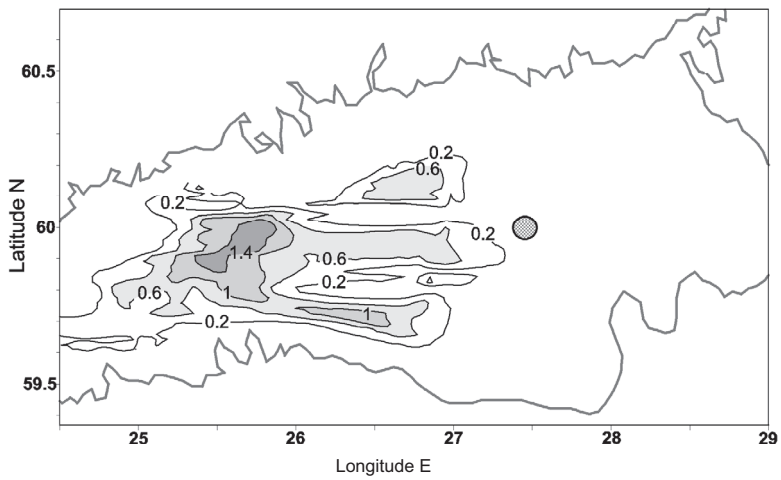

Fig. 6. Simulated daily growth rate of deformed ice in the Gulf of Finland on January 11, 2003. The unit at the contour interval is m/day. The circle denotes the location, where the ship damage occurred.

4.2. Ship damage on January 21, 2003

A tugboat 240 DWT, ice class IA, was damaged in the Gulf of Finland on January 21, 2003 due to the moving compressive ice field. The accident took place at the end of the lead, at the beginning of an ice field (about 60.15°N and 25.2°E). The ship stuck in ice field and started to drift along the ice masses with a speed of 2–3 knots. Ice pieces piled up against the ships side shell. The pile-up process and drifting lasted for about 20 min, then the compression ceased and ice pieces started to slide below the ship bottom; yet the ship had to wait for the icebreaker assistance [15].

Wind speed (Fig. 5) fluctuated from 2 to 7 m/s on 20–22 January. Higher speeds up to 10 m/s were observed earlier on 19 January. On 20 January, a day before the accident, wind turned from N to SW and then stayed in the southerly direction.

The observed ice thickness and concentration revealed large gradients in space on those days (Fig. 7). An ice lead extended from the western entrance in the northern part of the Gulf of Finland, with the ice thickness below 10 cm and concentration below 20%. In the eastern part of the central Gulf of Finland, the level ice thickness increased above 30 cm and the ice concentration above 90%.

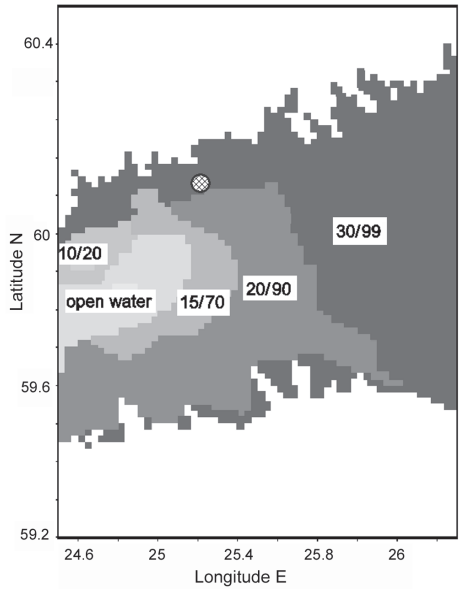

Fig. 7. Observed level ice thickness and concentration in the Gulf of Finland on January 21, 2003 (Finnish Institute of Marine Research, Ice Service). The circle denotes the location, where the ship damage occurred.

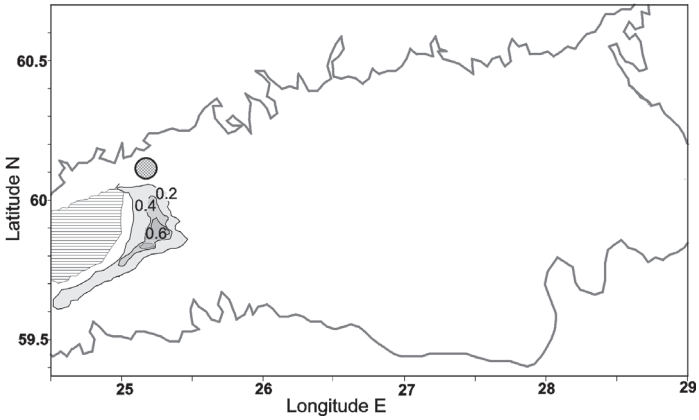

Fig. 8. Simulated growth rate of deformed ice in the Gulf of Finland on January 21, 2003. The unit at the contour interval is m/day. The hatched area denotes free water with ice concentration less than 10%. The circle denotes the location, where the ship damage occurred.

In the area, where ship damage occurred, the total ice concentration was about 70–99%. According to the model results, this area contained mostly deformed ice. The mean total ice thickness in the region was over 70 cm, whereas the mean ridged ice fraction was 60–80%.

Modelling results (Fig. 8) show that a strong deformation took place only in a small area to the south from the location of ship damage, at the edge of the ice margin. The northward drift of ice was the highest (14 cm/s) in the area with a low ice concentration, but at the northern border of the lead, the ice pack was almost motionless. This differential ice drift probably contributed to a high compressive stress in the ice pack. Like in the case of 11 January, the model simulations show only moderate (about 0.1 m/day) ridged ice production in the location of the accident, but much larger (0.6 m/day) ridging offshore.

5. DISCUSSION AND CONCLUSIONS

The Baltic Sea ice services are increasingly using operational ice models to support a safe and cost-efficient navigation. Among the ice-covered regions, the Gulf of Finland is of highest traffic intensity and unfortunately it has also the highest number of ship damages.

To the knowledge of the authors, this study is a first attempt to investigate if ship damage events are related to the ice field properties that can be simulated and forecast by the contemporary sea ice models. There are several generic sources of uncertainties in the process of constructing such models. Even with

the regional sea ice models, the model grid cells are significantly larger than the dimensions of ships, introducing the need to properly transfer the large-scale (1–2 km) ice field stresses into the forces that act on the hull of the ship. Stresses in the ice model are about 0.01 MPa (or with 1/3 m ice thickness 0.03 MPa), but on the much smaller scale in ship–ice impacts the stresses are of the order 1 MPa, in localized parts of hull even up to 70 MPa [29].

The study highlights the need of validation of the modelling of deformation events. In principle, an analysis of subsequent remote sensing images, results from a dense network of the ice drifters or measurements of the distribution of ice thickness could provide detailed enough information on the ice deformation for the model validation or data assimilation in order to improve the reliability of the model. However, retrieval algorithms of the motion and deformations of ice are still under development and all the regular ice monitoring observations are done in the fast ice region. As yet, neither the observed sea ice properties nor the modelled results can be applied to particular disasters with certainty. It is even unclear, which modelled parameters give an adequate forecast of the dangereous sea areas.

Our study showed that both the fraction of deformed ice (Fig. 4) and deformed ice thickness growth rate in the Gulf of Finland are smaller than in the Gulf of Riga. One might speculate that per unit of the icebound ship route (say 10^6 ship-km in ice) there could be more ice-related ship damages in the Gulf of Riga than in the Gulf of Finland. Scarce available data do not allow to make a reliable comparison. Comparison of data from different years allows to make some very rough estimates of the probability of damage. For example, 49 ice-related ship incidents [15] were reported in winter 2002/2003 and about 37 000 annual entrance crossings [1] in 2005/2006 in the Gulf of Finland. These numbers are 10 and 9000 for the Gulf of Riga. Therefore, about 1 incident per 200 ships entering or leaving each gulf occurs in the icebound conditions (that is, during 3 severe winter months).

We have selected two ship damage cases from the severe winter 2002/2003, when altogether 49 ice-related ship incidents occurred in the Gulf of Finland [15]. Unfortunately, in most of the cases (except the two under consideration), exact location and time of the damage event were missing. Therefore statistical analysis was not possible.

In both cases the ship damages happened close to the high growth rate area of deformed ice (Figs. 6 and 8) at the interface of different ice conditions with notable ice thickness gradients. Damages occurred when the ships were sailing in a region between the fast ice and intensive deformation areas in the open sea. The ridged ice production is an obvious indicator of the high compression of the ice pack. The areas, where ridging and rafting ice take place, may thus be considered as major risk regions for the wintertime navigation. The analysis suggests that quite large compressive forces occurred locally in areas relatively far from the intense compression regions. One may speculate that inhomogeneities in the ice (such as small leads or navigation channels) serve as favourable locations of

initiating of ridging even in relatively low overall compression rates. In the considered cases, ice deformations were additionally favoured by rapidly changing wind direction that apparently led to the formation of non-uniform patterns of ice drift.

ACKNOWLEDGEMENTS

This study has been carried out within the EC 6th Framework project SAFEICE (Increasing the Safety of Icebound Shipping) and supported also by Kristjan Jaak Foundation and by the Estonian Science Foundation (grant No. 5868).

REFERENCES

1. HELCOM. *Report on Shipping Accidents in the Baltic Sea Area for the Year 2005*. Baltic Marine Environment Protection Commission (Helsinki Commission), Helsinki, 2006.
2. Sonninen, S., Nuutinen, M. and Rosqvist, T. Development process of the Gulf of Finland mandatory ship reporting system. *VTT Publications*, Espoo, 2006, **614**.
3. Rytkönen, J. Risk review of the Baltic Sea shipping. In *Maritime Human Factors Research Group, Helsinki, 9–10 March 2006, VTT Presentations*. Espoo, 2006.
4. HELCOM. Towards a Baltic Sea with environmentally friendly maritime activities. In *2nd Stakeholder Conference on the HELCOM Baltic Sea Action Plan*. Helsinki, 2007. Baltic Marine Environment Protection Commission (Helsinki Commission), Helsinki, 2007.
5. HELCOM. *Recommendation 25/7 on Safety of Winter Navigation in the Baltic Sea Area*. Baltic Marine Environment Protection Commission (Helsinki Commission), Helsinki, 2004.
6. Seinä, A. and Palosuo, E. The classification of the maximum annual extent of ice cover in the Baltic Sea 1720–1995. MERI*: Report Series of the Finnish Institute of Marine Research*. Helsinki, 1996, **27**, 79–91.
7. Seinä, A., Eriksson, P., Kalliosaari, S. and Vainio, J. Ice seasons 2001–2005 in Finnish sea areas. MERI*: Report Series of the Finnish Institute of Marine Research*. Helsinki, 2006, **57**, 1–94.
8. Granskog, M., Kaartokallio, H., Kuosa, H., Thomas, D. N. and Vainio, J. Sea ice in the Baltic Sea – a review. *Estuarine Coastal Shelf Sci.*, 2006, **70**, 145–160.
9. Similä, M., Karvonen, J., Haas, C. and Hallikainen, M. C-Band SAR based estimation of Baltic Sea ice thickness distributions. In *Proc. IEEE International Geoscience and Remote Sensing Symposium, IGARSS 2006*. Denver, 2006.
10. Kankaanpää, P. Distribution, morphology and structure of sea ice pressure ridges in the Baltic Sea. *Fennia*, 1997, **175**, 139–240.
11. Lensu, M. *The Evolution of Ridged Ice Fields.* Helsinki University of Technology, Report M-280, Espoo, 2003.
12. Leppäranta, M. An ice drift model for the Baltic Sea. *Tellus*, 1981, **33**, 583–596.
13. Haapala, J., Meier, H. E. M. and Rinne, J. Numerical investigations of future ice conditions in the Baltic Sea. *Ambio*, 2001, **30**, 237–244.
14. Wang, K., Leppäranta, M. and Kõuts, T. A study of sea ice dynamic events in a small bay. *Cold Regions Sci. Technol.*, 2006, **45**, 83–94.
15. Hänninen, S. Incidents and accidents in winter navigation in the Baltic Sea, winter 2002–2003. *Finnish Maritime Administration Research Report*, Helsinki, 2003, **54**.

16. Haapala, J. Evaluation of the sea-ice components of the ACIA Atmosphere-Ocean General Circulation Models (AOGCMs). In *Arctic Climate Feedback Mechanisms: Proc. Workshop at the Norwegian Polar Institute* (Gerland, S. and Njåstad, B., eds.). Tromsø, Norway, 2003. *Norsk Polarinstitutt Rapportserie*, Tromsø, 2004, **124**, 19–21.
17. Haapala, J., Lönnroth, N. and Stössel, A. A numerical study of open water formation in sea ice. *J. Geophys. Res*., 2005, **110**, C09011.
18. Thorndike, A. S., Rothrock, D. A., Maykut, G. A. and Colony, R. The thickness distribution of sea ice. *J. Geophys. Res*., 1975, **80**, 4501–4513.
19. Hibler III, W. D. Ice dynamics. In *Geophysics of Sea Ice* (Untersteiner, N., ed.). *NATO ASI Series B, Physics*, vol. 146, Plenum Press, New York, 1986, 577–640.
20. Parmeter, R. R. A model of simple rafting in sea ice. *J. Geophys. Res.*, 1975, **80**, 1948–1952.
21. Rothrock, D. A. Modeling sea-ice features and processes. *J. Glaciol.*, 1979, **90**, 359–375.
22. Timco, G. W. and Burden, R. P. An analysis of the shapes of sea ice ridges. *Cold Regions Sci. Technol.*, 1997, **25**, 65–77.
23. Hibler III, W. D. A dynamic thermodynamic sea ice model. *J. Phys. Oceanogr*, 1979, **9**, 815–846.
24. Rothrock, D. A. The energetics of the plastic deformations of pack ice by ridging. *J. Geophys. Res.*, 1975, **80**, 4514–4519.
25. Zhang, J. and Hibler III, W. D. On an efficient numerical method for modeling sea ice dynamics. *J. Geophys. Res.*, 1997, **102**, 8691–8702.
26. Pastukhov, G. and Talijev, D. *Brief Information on Ice Conditions in Gulf of Finland in the Winter 2002–2003*. NW Administration of Federal Service of Russia for Hydrometeorology and Environmental Monitoring (NW Hydromet), St. Petersburg, 2003 (in Russian).
27. Haas, C. *Airborne EM Measurements of Baltic Ice Thickness*. IRIS data report, Alfred Wegener Institute for Polar and Marine Research (AWI), Bremerhaven, Germany, 2003.
28. Pärn, O. and Haapala, J. Analysis of the ice model simulation for the Gulf of Finland in 2002/03. *Geophysica*, 2007. Forthcoming.
29. Jordaan, I. J. Mechanics of ice-structure interaction. *Eng. Fract. Mech.*, 2001, **68**, 1923–1960.

Soome lahe jäädeformatsiooni ja laevavigastuste vahelisest seosest 2003. aasta talvel

Ove Pärn, Jari Haapala, Tarmo Kõuts, Jüri Elken ja Kaj Riska

Rüsijää ahelikud ja ladejää on talvisel meresõidul peamisteks takistusteks. Tuulte põhjustatud jäätriiv tekitab pinged jääkattes, mis kutsub esile suuri jää moondeid. Soome laht on Läänemere ohurikkamaid piirkondi, kus 2002/2003. aasta talvel toimus ligikaudu 60% laevavigastustest. Artiklis on analüüsitud numbrilise jäämudeli (HELMI) väljundandmeid, seostades deformeerunud jää paksuse kasvu kiiruse kahe sel talvel juhtunud laevavigastusega. Mõlemad avariid juhtusid erinevate jääliikide üleminekualal, kus esines märkimisväärne deformeerunud jää paksuse kasv.

Paper II

Pärn, O. & Haapala, J. 2011. Occurrence of synoptic flaw leads of sea ice in the Gulf of Finland. *Boreal Environ. Res.*, 16(1), 71–78.

BOREAL ENVIRONMENT RESEARCH 16: 71–78
ISSN 1239-6095 (print) ISSN 1797-2469 (online)

Helsinki 28 February 2011

Occurrence of synoptic flaw leads of sea ice in the Gulf of Finland

Ove Pärn[1] and Jari Haapala[2]

[1)] *Marine Systems Institute at Tallinn University of Technology, Akadeemia tee 21, EE-12618 Tallinn, Estonia (kylmleek@gmail.com)*
[2)] *Finnish Meteorological Institute, Erik Palménin aukio 1, FI-00560 Helsinki, Finland*

Received 18 Oct. 2009, accepted 16 June 2010 (Editor in charge of this article: Kai Myrberg)

Pärn, O. & Haapala, J. 2011: Occurrence of synoptic flaw leads of sea ice in the Gulf of Finland. *Boreal Env. Res.* 16: 71–78.

In spite of their importance to the marine ecosystem and winter navigation, flaw leads have not received much attention. This study presents an analysis of the flaw lead occurrence frequency in the Gulf of Finland. We used ice charts of the Estonian Meteorological and Hydrological Institute covering the years 1971–2007 and the Helsinki multi-category sea-ice model. Flaw leads are formed in the Gulf of Finland almost everywhere along the fast-ice edge when moderate or strong winds are acting, but the winds from W, NW, N and S sectors generate a rather uniform lead pattern, thus facilitating navigation in the ice. On average, flaw leads are most common in the Estonian coastal region where their occurrence is typically 10%–30%. However, during severe winters when northerly winds are more frequent flaw leads are also common in the Finnish coastal region.

Introduction

On the synoptic scale, sea-ice conditions are variable and rapidly changing. Pack ice can drift over 25 km during a stormy day. In a large restricted basin, such as the Gulf of Finland (GoF), sea-ice drift has large horizontal gradients due to the vicinity of landlocked fast ice, causing sea-ice ridging in the compressive regions and opening of pack ice in the divergent regions. A prominent site-specific feature of this differential ice drift is flaw lead, which is defined as open water between pack ice and fast ice. These weather-dependent, synoptic flaw leads are observed frequently in the GoF and in some cases the open water area can extend over several hundred kilometers.

Generation of flaw leads enhances heat and moisture exchange between the atmosphere and the ocean, leading to increased fogging and precipitation in the atmosphere and intensified vertical mixing and ventilation in the ocean. It is especially important in the Arctic Ocean in the regions of perennial sea-ice cover, where flaw leads have quite often a large extent and duration (Kassens 1994) and have important consequences for functioning of the marine ecosystem.

In the Arctic, the Laptev Sea is a region where flaw leads are commonly observed. Dynamics of flaw leads were first studied by Zakharov (1966). Later, Dethleff (1994), Dethleff *et al*. (1998) and Liu *et al*. (2009) showed that the Laptev Sea flaw lead is driven by hydrometeorological factors and bathymetry. A very long lead (approximately 2000 km long) lies at up to 30 m water depth, bordering the coastal fast ice. The width of the open water ranges from 100 m to 25 km depending on synoptic winds. The flaw lead favors circulation of deep and near-bottom waters. It has

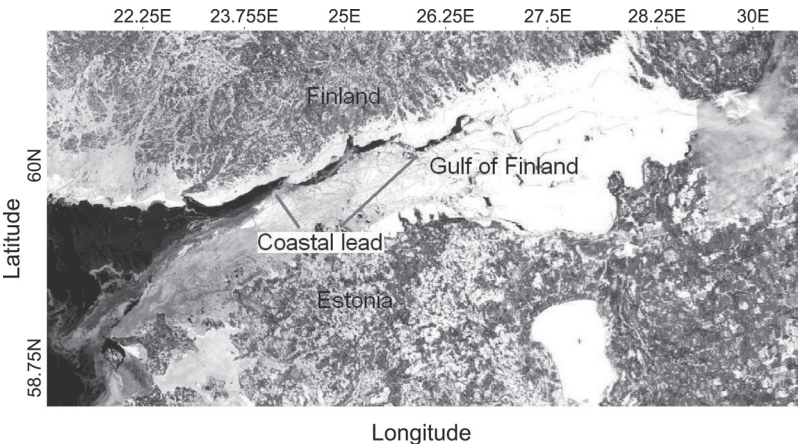

Fig. 1. Ice situation in the Gulf of Finland on 20 January 2003 (Moderate Resolution Imaging Spectrometer image by Liis Sipelgas). Observed situation was preceded moderate NW and N winds on 19 and 20 January.

also environmental effects like enhanced sediment transport (Stein and Korotov 1994).

Flaw leads are also natural fairways for vessels navigating in ice (Fig. 1). Although this aspect is not widely explored in scientific literature, in practice seafarers tend to utilize flaw leads whenever possible. In enclosed basins with seasonal ice cover, the shipping aspect of flaw leads in local economy is apparently more important than the impacts of leads on the regional climate are.

The GoF is one of the most intensive shipping regions in the world (Sonninen *et al*. 2006). During the last decade, oil transportation from Russian terminals has increased remarkably, intensifying essentially the tanker traffic along the GoF. This tendency is predicted to continue, and much attention has been paid to navigational safety, especially in winter, both on scientific and management levels (HELCOM 2007).

Under average winter conditions, ships have to navigate in the Baltic Sea at least 150 nautical miles in ice-covered waters, while during a very severe winter, the ice-sailing distance can exceed 400 nautical miles (Seinä and Palosuo 1996). Some ice forms even during mildest winters. The ice season begins usually in December when the shallow coastal regions are frozen in the easternmost GoF. On average, the ice season lasts until the middle of April, but in small bays sea ice remains until May. In winter, sea ice shoud be considered a primary factor causing ship damages that may result in pollution.

Flaw leads in the Baltic have not yet been studied much. The only published study so far was conducted by Haas (2004), who carried out detailed ice thickness measurements along the whole Finnish coastline in February 2003 using the helicopter-borne electromagnetic-inductive (HEM) method. The flaw lead detected in the GoF was surrounded by thick deformed ice (up to 5 m) between Helsinki and Tallinn. The flaw leads, detected by the HEM method, were in general well visible also on the routine ice charts.

The objective of this work is to analyze the occurrence frequency of flaw leads in the GoF. We analyze EMHI (Estonian Meteorological and Hydrological Institute) ice charts and utilize the Helsinki multi-category sea-ice model in order to study the appearance of leads and determine how lead formation depends on the large-scale wind direction.

Material and methods

Observational data

This study is based on the ice charts covering the period 1971–2007. The ice charts used here were compiled by the EMHI using their own observations as well as the charts of the Finnish Ice Service and the Russian ice charts, which rely largely on satellite data and visual observations from air, land and ships. Every chart represents the ice distribution over the GoF on a particular date.

Here, in surveying and analyzing the ice charts, the flaw lead is defined as a narrow linear

region of open water, new ice or region of low ice concentration that is located either between two areas of compact ice or between pack ice and fast ice.

The ice charts were converted into matrixes for every date (an example matrix for 22 February 1996 is presented in Table 1). The data on the distribution of wind direction in the middle of the GoF (Fig. 2) are based on the NCEP/NCAR reanalysis. In spite of the coarse resolution of the NCEP/NCAR data, they describe average wind conditions in the Baltic Sea area very well: the correlation coefficient between the NCEP/NCAR data and surface observations is 0.91 for zonal and 0.88 for meridional components of the wind (Pärn and Haapala 2007).

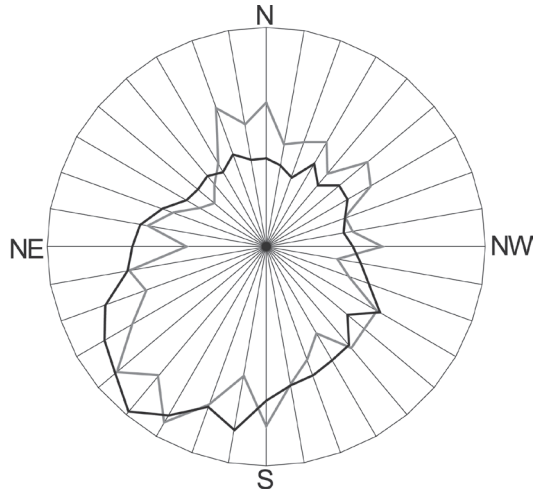

Fig. 2. Directional frequency distribution of the winds with daily speed over 4 m s^{-1} in winter (January–April). Data from 1971–2007 for the middle of the Gulf of Finland. Black line in the rose indicates average winter and grey line severe winter.

Model experiments

The HELMI (HELsinki Multicategory Ice model) model used in this study, resolves ice thickness distribution, i.e. ice concentrations of different thickness categories, redistribution of ice categories due to deformations, thermodynamics of sea ice, horizontal components of ice velocity and internal stress of the ice pack. An ice pack is a mixture of open water and undeformed and deformed ice categories of variable thickness. Deformed ice is separated into rafted- and ridged-ice classes. The model has been used in large-scale studies (Haapala *et al*. 2005) and operational applications. The model physics and numerics are the same for both operational and climate simulations. The only differences are in the horizontal resolution and atmospheric data used for calculations of surface heat and momentum fluxes.

The present setup of the sea-ice model simulated evolution of five undeformed and two deformed ice categories. Ice categories are not restricted to any particular ice thicknesses except for the thinnest ice-thickness category that is not allowed to exceed 10 cm. Deformed ice is divided into two categories: rafted ice and ridged ice. The horizontal resolution of the model is 1 nautical mile.

Observed ice deformations: leads with respect to navigability

An example of an individual ice chart, avail-

Table 1. Ice chart (Fig. 3) converted into a matrix. 0 stands for ice cover and 1 stands for open water, new ice or a region of a low ice concentration.

	23°–24°E	24°–25°E	25°–26°E	26°–27°	27°–28°E	28°–29°E	29°–30°E
60°30´–60°20´N	0	0	0	0	0	0	0
60°20´–60°10´N	0	0	0	1	0	0	0
60°10´–60°00´N	0	0	1	1	0	0	0
60°00´–59°50´N	0	1	0	0	0	0	0
59°50´–59°40´N	1	0	0	0	0	0	0
59°40´–59°30´N	0	0	0	0	0	0	0
59°30´–59°20´N	0	0	0	0	0	0	0
59°20´–59°10´N	0	0	0	0	0	0	0

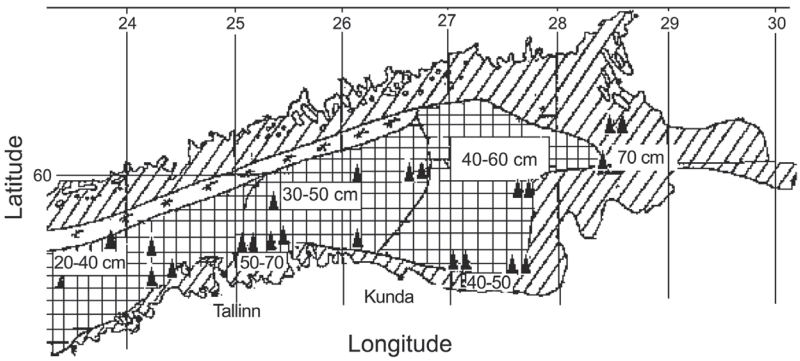

Fig. 3. The EMHI ice chart for the date of the largest ice extent (22 February 1996) in the ice season 1995/1996. During the previous few days winds blew alternately from N, NE and NW. The triangles indicate ridged ice, diagonal lines fast ice and squares consolidated ice.

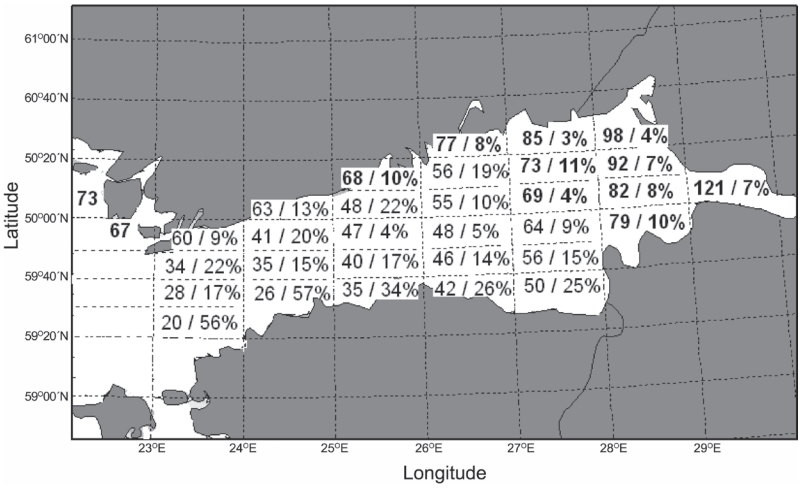

Fig. 4. Average ice conditions in the Gulf of Finland during 1971–2007 in the 1.0° long. × 0.2° lat. grid. The first number in the cells is the average duration of the ice cover in days, and the second is the ice lead occurrence expressed as the percentage of the ice days.

able from the EMHI database, is given in Fig. 3. During the maximum ice extent, ridged ice covers large offshore areas of the GoF, and ice thickens towards the east. Ice is ridging more severely in the narrowest part of the GoF between 25°E and 25°30´E and in its widest part between 27°E and 28°E. Also notable differences in ice properties in the north–south direction are evident. As strongest winds blew from NW, N and NE before 22 February — that is prior to the generation of the ice chart (Fig. 3) — ice drifted southwards generating a lead about 10–20 km from the Finnish coast. In the compressive region to the south and east of landfast, ice ridges were formed.

The ice-cover period and the occurrence of leads (percentage of ice days) in different regions of the GoF were calculated from the ice charts covering the period 1971–2007. The statistics was calculated for the regular 1.0° long. × 0.2° lat. grid.

We also examined which areas are favorable for navigation and harbors, assuming a low ice concentration allows flaw leads to favor shipping, whereas the regions of high ice concentration are typically also regions of deformed ice, which are obstacles to navigation.

The occurrence of leads is the most common in the Estonian coastal area, where their occurrence is typically 10%–30% (Fig. 4). In the middle of the GoF, leads make up a much smaller percentage. For example, between 25°E and 26°E, the lead occurrence was only 4% in the middle of the basin, whereas it increased to 22% at the Finnish coast and to 34% at the Estonian coast. The lead occurrence was highest at the entrance to the GoF due to thin ice — a result of a short ice-cover period — as well as ice-cover disturbance caused by winds and sea currents.

In order to find the relationship between the wind direction and the spatial pattern of the lead occurrence, we calculated wind distributions for

days when the daily wind speed exceeded 4 m s^{-1} as lower wind speeds are not expected to cause ice drift. The analysis revealed that moderate and strong winds blew mostly from SW. The frequency of winds from the S–W sector was 37%, while those from the opposite sector (between N to E) was only up to 21%.

Results of the numerical analyses

We estimated how the ice deformation rate and open water formation are related to wind direction and how these vary at a regional scale. The results are based on the idealized numerical analyses, in which sea ice was initially constant: the level ice thickness was set to be 0.35 m, the ice concentration A = 0.99. Then the response of the sea-ice model to constant, 10 m s^{-1} wind from different directions was calculated.

In order to analyze which wind directions facilitate navigation in ice, we assumed that in those regions where the modeled ice concentration was below 85%, the ships could navigate without any difficulties. The grid points with a low ice concentration were considered equivalent to flaw lead areas.

Under northerly winds, an extensive flaw lead, parallel to the coastline, extended from the mouth to the end of the GoF (Figs. 1 and 5a). In that case, vessels could easily navigate in the Finnish coastal zone. However, the picture was quite different under north-easterly winds. This wind situation also generated much open water, but contrary to the previous case, open water areas were separated by an island, and uniform lead was generated only in the easternmost part of the GoF (Figs. 5b and 6). Such a situation was observed on 22 February 1996, when — due to NW, N and NE winds on the previous day — a lead occurred throughout the GoF from the estuary (23°E) to almost the middle of the ventrix (27°E) (Fig. 3).

Also southerly winds, blowing transverse to the basin, were favorable for the flaw lead generation (Fig. 5). In this case, the lead was located by the Estonian coast reaching from the mouth (23°E) to the central part of the GoF (28°E), while a few minor leads did exist by the Ingerian (southern) shore of the GoF (between 28°E and 29°E). The EMHI ice charts for 1971–2007 show that leads appeared quite often near the Estonian coast (Fig. 4). Thus the model results reflect well the empiric data.

Southwesterly winds were the most common in winter (Fig. 2). In those cases, a minor lead was formed near the Estonian coast in the middle of the GoF (Fig. 5f).

During flaw-lead formation events, sea ice was ridging and thickening in some regions of the GoF. To estimate the mean thickness of deformed ice, the thickness was integrated over the latitude L (59°25´N–60°30´N). The latitude-integrated deformed ice thickness is

$$H = \frac{1}{L}\int_{L_1}^{L_2} \tilde{h} dL,$$

where $\tilde{h}$ is the mean deformed ice thickness in the model grid (Haapala *et al*. 2005). Figure 7 presents how the mean deformed ice thickness varied in space and is thickening in time under an action of the SW wind. After five hours of the SW wind action, the deformed ice grew over 0.01 m thicker at the longitudes 24°30´, 25°30´, 27°, 28°, 28°30´E. Further, we can see that deformed ice grew 0.07–0.1 m thicker per day in those regions, whereas between these areas the deformed ice grew less than 0.01 m during the same time.

Discussion and conclusions

The presence of sea ice in the GoF for 3–5 months each winter is a challenge for winter navigation. Flaw leads, as natural waterways, can greatly facilitate shipping. In this work, we examined the frequency of flaw leads based on daily ice charts and modeled ice conditions to study how lead formation depends on wind.

Flaw leads are a common feature in the GoF. Practically winds from all directions generate open water and leads in pack ice, but winds from W, NW, N and S in particular form a rather uniform lead pattern thus facilitating navigation in the ice (Fig. 8). This is important during severe winters when the GoF is fully covered by thick and ridged ice.

On average, flaw leads were the most common in the Estonian coastal region. How-

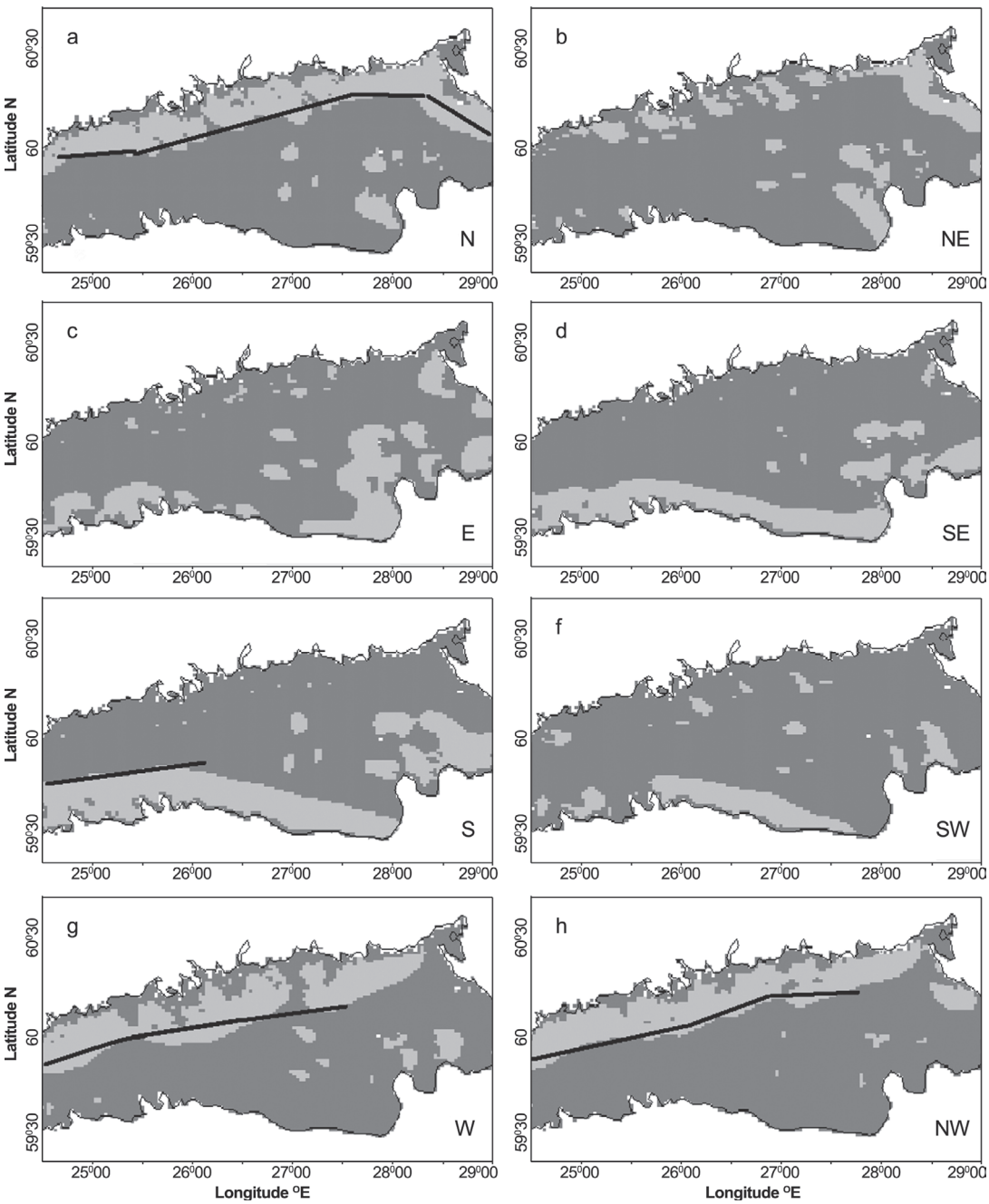

Fig. 5. The modeled occurrence of leads during different wind conditions in the Gulf of Finland. Light grey indicates the lead and dark grey indicates an area fully covered by ice. The line shows an optimal route of a vessel navigating in ice.

ever, during severe winters, northerly winds were more frequent and therefore also flaw leads were common in the Finnish coastal region. Under certain conditions, the same dominant wind direction could prevail for several weeks, leading to a situation that flaw lead is extended as far as the middle of the basin.

Concurrent with generation of flaw leads, drift ice is also compacting and ridging in the opposite side of the basin. In order to show how

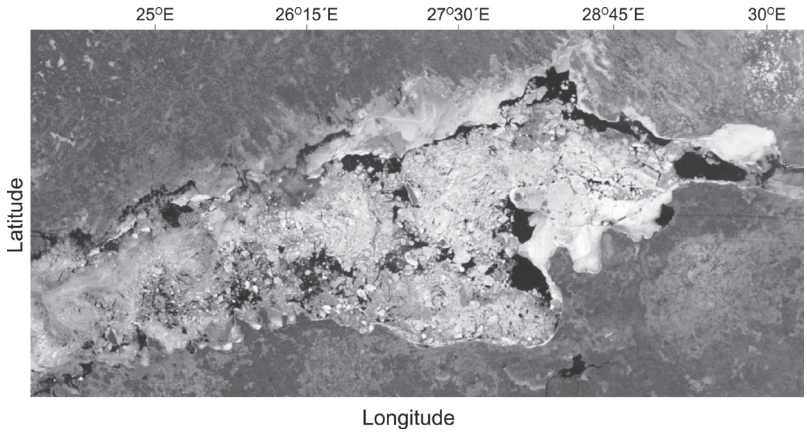

Fig. 6. Ice situation on 20 April 2003. On 19 and 20, April the wind blew from NNE and N with speeds of 0–2 m s^{-1}, on 18 April the speed of the NE wind was 4–8 m s^{-1}. Consequently, generated ice-free regions are patchy.

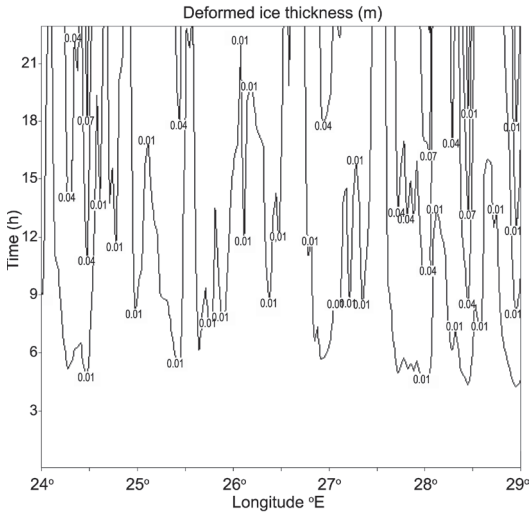

Fig. 7. The mean thickness of deformed ice as a function of longitude and time after the onset of constant SW wind of 10 m s^{-1}, starting from the horizontally homogeneous ice conditions.

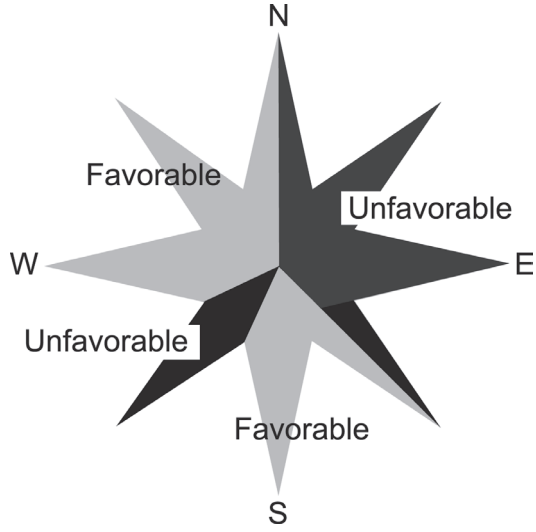

Fig. 8. Ice conditions favoring vessel navigation form along the Gulf of Finland when a constant wind blows for at least 10 h. W, NW, N and S winds generate a rather uniform lead pattern, thus facilitating navigation in the ice.

important the mechanical thickening of ice is, we can compare growth rates the deformed ice with the thermodynamic growth rate of ice. If the air temperature is –10 °C, then 0.35-m thick ice grows by about 0.01 m per day. Thus the thermodynamic growth rate of undeformed ice is slow as compared with that of the deformed ice since in the same conditions, the new ice in the leads is thickening by about 0.05 m per day.

The ship damage risk is higher closer to the areas of high ice deformation rate where ice floes of different properties meet, yielding also a clear ice thickness gradient (Pärn *et al*. 2007). Such situations occur when navigating from an area of low-concentrated ice to an area of high-concentrated thick, probably ridged ice. The present study enables for a rough estimate of the navigation conditions based on the weather forecast and gives a few general guidelines for selecting the routes under severe ice conditions.

Acknowledgments: This study was supported by the Estonian Science Foundation (grant no. 7328). We wish to thank the Estonian Meteorological and Hydrological Institute (Kai Loitjärv, Riina Vahter) and Liis Sipelgas, who shared with us SAT images.

References

Dethleff D. 1994. Dynamics of the Laptev Sea flaw lead. *Ber. Polarforsch*. 144: 49–54.

Dethleff D., Loewe P. & Kleine E. 1998. The Laptev Sea flaw lead — detailed investigation on ice formation and export during 1991/1992 winter season. *Cold Reg. Sci. Technol*. 27: 225–243.

Haapala J., Lönnroth N. & Stössel A. 2005. A numerical study of open water formation in sea ice. *J. Geophys. Res*. 110: C09011.1–C09011.17.

Haas C. 2004. Airborne EM sea-ice thickness profiling over brackish Baltic Sea water. In: *17th International Symposium on Ice, International Association of Hydraulic Engineering and Research*, Saint Petersburg, pp. 12–17.

HELCOM 2007. Towards a Baltic Sea with environmentally friendly maritime activities. In: *2nd Stakeholder Conference on the HELCOM Baltic Sea Action Plan*, Helsinki, pp. 5–25.

Kassens H. & Thiede J. 1994. Climatological significance of Arctic sea ice at present and in the past. *Ber. Polarforsch*. 144: 81–86.

Liu C., Chang Y.-C., Huang S., Yan S.-Y., Wu F., Wu A.-M., Kato S. & Yamaguchi Y. 2009. Monitoring the dynamics of ice shelf margins in Polar Regions with high-spatial- and high-temporal-resolution space-borne optical imagery. *Cold Reg. Sci. and Technol*. 55: 14–22.

Pärn O. & Haapala J. 2007. Analysis of the ice model simulation for the Gulf of Finland in 2002/03. *Ber. Bundesamt. Seesch. Hydrogr.* 42: 37–45.

Pärn O., Haapala J., Kõuts T., Elken J. & Riska K. 2007. On the relationship between sea ice deformation and ship damages in the Gulf of Finland in winter 2003. *Proc. Estonian Acad. Sci. Eng*. 13: 201–214.

Seinä A. & Palosuo E. 1996. The classification of the maximum annual extent of ice cover in the Baltic Sea 1720–1995. *Meri* 27: 79–91.

Sonninen S., Nuutinen M. & Rosqvist T. 2006. Development process of the Gulf of Finland Mandatory Ship Reporting System. *VTT Publ*. Espoo, pp. 12–30.

Stein R. & Korolev S. 1994. Shelf-to-basin sediment transport in the eastern Arctic Ocean. Russian–German cooperation in the Siberian shelf seas: geo-system Laptev–Sea *Ber. Polarforsch*. 144: 87–100.

Zakharov V.F. 1966. The role of flaw leads off the edge of fast ice in the hydrological and ice regime of the Laptev Sea. *Acad. Sci. USSR* 6: 815–821.

Paper III

Pärn, O., Haapala, J. & Sipelgas, L. 2010. Leads as natural fairways in the Gulf of Finland. Baltic International Symposium (BALTIC), 2010 IEEE/OES US/EU, 1 – 7, doi: 10.1109/BALTIC.2010.5621638

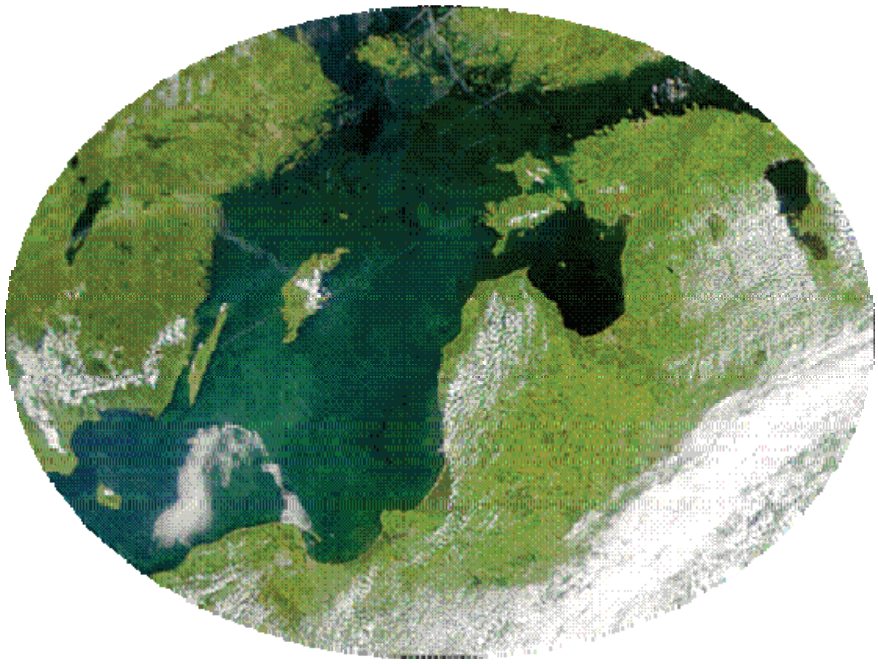

2010 IEEE/OES US/EU Baltic International Symposium (BALTIC)

August 25, 26, 27 2010 - Riga, Latvia

IEEE Catalog Number: CFP10AME-ART
ISBN: 978-1-4244-9227-5/10/$26.00 ©IEEE

Leads as natural fairways in the Gulf of Finland

Ove Pärn[1], Jari Haapala[2] and Liis Sipelgas[1]

[1]Marine Systems Institute at Tallinn University of Technology, Akadeemia tee 21, 12618 Tallinn, Estonia; kylmleek@gmail.com

[2]Finnish Meteorological Institute, Erik Palménin aukio 1, FIN-00560 Helsinki, Finland; jari.haapala@fmi.fi

Abstract – **The monitoring and prediction of sea ice conditions are vital for safe and economical winter navigation in the Gulf of Finland (GoF), where ice conditions are very variable and dynamic. Flaw leads and ice ridges are common features in the GoF. In this study the occurrence frequency of the leads and ridges during 1971-2009 is analyzed. For the historical period, the ice charts of the Estonian Meteorological and Hydrological Institute (EMHI) were used for determining their occurrence and location in the Gulf of Finland. A case study was performed for a severe winter in 2002/2003. MODIS satellite imagery was used in addition to ice charts for determining the location of the leads in the Gulf of Finland. Also, the HELMI ice model was used to examine ice characteristics during the winter of 2002/2003 and the relationship between deformed ice growth rates and the speed and direction of wind. The results of the analysis of historical data show that on the average the leads are most common in the Estonian coastal region where their occurrence is typically 10-30%. During severe winters, leads occur quite often also in the Finnish coastal region, but the ridges are more common in the Estonian coast.**

I. INTRODUCTION

The GoF is one of the most intensive shipping regions in the world [1]. Wintertime navigation is continuously increasing and it is expected to double by 2015. A lot of attention is paid to navigation safety, especially with respect to winter navigation, on both the scientific and management level, seriously considering many environmental concerns [2-4]. In 2002 the European Union (EU) set up the IRIS project "Ice Ridging Information System for Decision Making in Shipping Operations". Ice modeling and satellite imagery (Synthetic Aperture Radar) interpretation is being developed to include sea ice characteristics in navigation information so that enhanced ice information could be applied on selected ship routes. The SAFEICE project of the EU studied ship-ice interaction and analyzed ice damages that occurred in the Gulf of Finland. In 2010, the EU launched the SAFEWIN project on Safety of Winter Navigation in Dynamic Ice. This project aims to develop an efficient ice compression and ice dynamics forecasting system.

Ice conditions increase considerably resistance on the ship even in calm weather and they have to be taken into account during winter navigation to choose the optimal navigation route. In dynamic ice conditions one needs different paths to the same destination, thus having various path lengths and passing times. The criteria for optimizing navigation routes were investigated by Kotovirta et al [5].

Blowing wind modifies ice conditions essentially by raising stress in an ice field, resulting in compressive deformation of ice. Some ice fields can be significantly deformed even by a wind of 4 m/s if it blows from a suitable direction [6]. Both the ice stress itself and ice deformation endanger a vessel navigating in ice. During the severe winter of 2002/2003, ca 62% of ship hull damages over the Baltic Sea occurred in the Gulf of Finland. 30% of the damages were caused by ship-ice interaction and 15% of them occurred in a compressive ice field [7].

Openings in ice are a common feature in the GoF. A flaw lead is an area of open water between pack ice and fast ice. An open water area can sometimes extend over several hundred kilometers. If a lead lies along the GoF axis, it facilitates the navigation through the area. The impact of such leads and other openings on a vessel in the GoF is studied by Pärn and Haapala [8]. In the GoF the W, NW, N and S winds generate leads that are wide enough for a vessel to navigate through. This is particularly important with regard to severe winters when the GoF is fully covered with thick and ridged ice. Previous studies have shown that during average winters, the leads are more common in the Estonian coastal region [8]. But during severe winters the northern winds blows more frequently and thus we have more flaw leads in the northern part of the gulf.

The historical ice conditions over the GoF have been studied by several authors [9-11]. The time series of the climate characteristics indicate three winter types: the mild, the average and the severe. The Gulf of Finland is fully ice-covered in normal and severe winters, some areas of the gulf freeze even in very mild winters. Ice forms first in the eastern part of the gulf already in the beginning of December and usually melts in the middle of April [9]. In the coastal zone and small bays ice can last even until the beginning of May. Ice-covered periods can last longer in the eastern part of the GoF and less in the western entrance area. The level ice in the GoF is typically 30–40 cm thick, but in certain snow-free conditions it may reach up to 80 cm. Ridging in the GoF is frequent – the portion of ridged ice is usually 25% as from February [12]. Ice ridges in the GoF are typically 5–10 m thick.

For safe navigation in the GoF we must first consider severe winters. To enhance winter navigation safety it is useful to study both the large-scale and the local characteristic features and processes of the ice. General analysis describes only gross patterns of ice characteristics, but local analysis takes into account specific information about the vessel size and location to estimate the influence of ice to a vessel. The local scale processes occur under the multiple interacting factors. The resulting stochastic events quite often cannot be predicted with a satisfactory confidence.

The paper aims to study the impact of weather and ice features on winter navigation in the GoF during severe winters. Basically, the leads are facilitating shipping and the ridges and other deformed ice regions are hindrances to the navigation.

The occurrence frequency of the leads and ridges was analyzed in various areas of the GoF during ice seasons in 1971–2009. For this period the EMHI (Estonian Meteorological and Hydrological Institute) ice charts were used to identify the presence and location of ridged and rafted ice and leads in the Gulf of Finland. A case study was performed for the severe winter of 2002/2003. In addition to the ice charts, we used the MODIS satellite imagery to determine the leads distribution over the GoF. Also, the HELMI ice model was used to examine ice characteristics during 2002/2003 and to learn how deformed ice growth rates are related to wind speed and its direction.

II. Materials and methods

A. Observational data

The current study is based on ice charts from the period of 1971–2010. The ice charts originate from EMHI. These charts are compiled relaying on Finnish Ice Service ice charts, Russian Ice Service ice charts and from satellite observations as well as visual observations from air, land and ships. Every chart represents ice distribution over the GoF at a particular date.

Analyzing the ice charts, the lead was defined as a narrow linear region of open water, new ice or a region of low ice concentration located either between two areas of compact ice or between pack ice and fast ice. All daily charts were converted into the gridded form and ice characteristics for each grid cell were identified.

B. Model experiments

We applied the HELMI (HELsinki Multicategory Ice) model for this study. The model resolves ice thickness distribution, i.e. ice concentrations of different thickness categories, redistribution of ice categories due to deformations, thermodynamics of sea-ice, horizontal components of ice velocity and internal stress in ice pack. An ice pack is a mixture of open water and level ice and deformed ice categories of variable thickness. Deformed ice is divided into the rafted ice and ridged ice classes. The model has been used in large-scale studies [13] and operational applications. The model physics and numerics are the same both in operational and climate simulations. The only differences are the horizontal resolution and the scheme of atmospheric forcing used.

The present set-up of the sea ice model predicts the evolution of five level ice and two deformed ice categories. Ice categories are time-stepped in the thickness space without any limits, except the thinnest category that is not allowed to exceed 10 cm in thickness. The horizontal resolution of the model is 1 nautical mile (1.852 km).

III. The impact of leads and ice deformation rates on the navigability as estimated by the ice dynamics model and as observed

A. Natural conditions in the severe winter of 2002/03

The winter of 2002/2003 stands out as a very severe winter in terms of the length of ice-covered period and thickness of ice cover in the GoF. In comparison with the average, the ice-covered period lasted longer by one month. The cold season began early in the autumn in 2002 and temperature remained below the average for most of November and December. Ice-cover records show a significant ice thickness already in December. The winter of 2002/2003 is stated to be one of the coldest over the last 34 years (except the winter of 2009/2010 that awaits a proper examination).

In November 2002 the ice cover started to form rapidly in the eastern part of the GoF. Ice had covered the entire GoF by the end of the year. Ice thickness was 50 cm in the eastern parts of the GoF and about 15 cm on the western side [14]. By the end of January 2003, the thickness of ice grew up to 80 cm on the Finnish coast.

The length of a sea lane that ships go through ice in the GoF is usually about 100 km, but in the winter of 2002/2003 it reached up to 400 km due to difficult navigation conditions. The ice-breaking period was then significantly longer than during an average winter. In 2003 ice was very thick and deformed, navigation was difficult and navigational restrictions were valid for 117–149 days [15]. Ice breaking is usually first needed in January, but during that winter icebreaking in the GoF started already in December.

For the studied year (2002/2003) the mean deformed ice growth rate was modeled in the Gulf of Finland. The mean deformed ice concentration was up to 40% of the total ice-covered area. A relationship between ship damages and deformed ice growth rate was analyzed (Fig 1). On 15–18.01.2003 wind induced considerable ice deformation near the northern shore. At that time 8 accidents took place, where the ship hull was damaged by the ice. Also, a significant growth rate of deformed ice occurred on 27–28.02 and at that time 5 ship accidents happened [7]. During the rest of the ice season the damage occurrence rate did not exceed 1 per day.

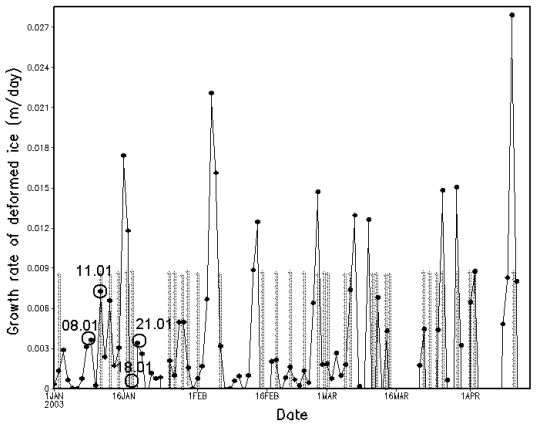

Figure 1. The mean growth rate of deformed ice and the dates when ship damages took place in the winter of 2002/03. Ship damage dates are marked with vertical lines. The mean deformed ice growth rate is calculated over the entire Gulf of Finland. Ship damages are marked with the vertical line and the circles denote the damage events known to be caused by compressive ice [7].

We also analyzed how ice deformation rates relate to wind speed and wind directions in the winter of 2002/2003. As can be seen from Fig. 2, wind speed alone does not determine the ice deformation rate and wind direction is crucial in generating deformation. Fig. 2 shows that the E, S and NW winds tend to cause the most powerful deformation rate.

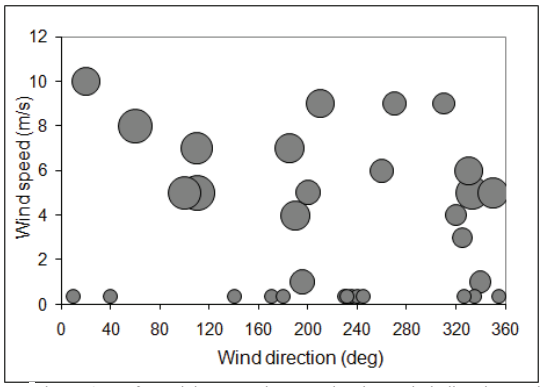

Figure 2. Deformed ice growth rate related to wind direction and speed. The circles denote the average (over GoF) growth rate from 0.07 m/day to 0.18 m/day as shown by the circle diameter.

We analyzed the cumulative deformation phenomena (ridging and rafting) impeding winter navigation. According to the model calculations, more than 60% of the ice deformation events took place in the southern part of the GoF. Also, the mass of deformed ice was greater in the southern part (Fig. 3) and the deformation was twice as strong on the southern coast than on the northern one. For example, at 60.20`N, the average deformed ice thickness was 0.2 m, whereas at 59.30`N it was 0.5 m over the level ice.

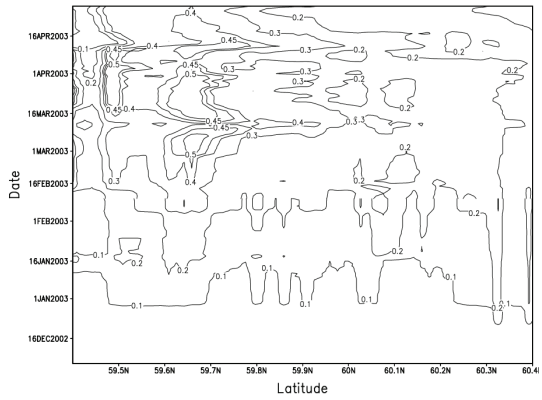

Figure 3. The development of deformed ice thickness in various latitude sections. To characterize each section, the modeled deformed ice thickness is integrated over the latitude (along the parallels).

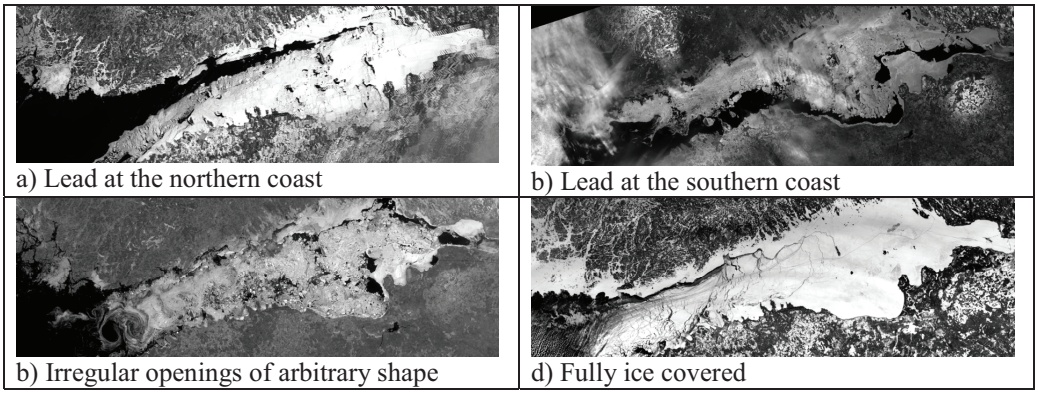

Figure 4. Ice situation in the GoF in 2003. Moderate Resolution Imaging Spectrometer images (Modis).

As mentioned earlier, leads enable shipping through ice. To investigate the occurrence of such openings we studied MODIS satellite images from the year 2003. Altogether 51 images were analyzed and the results are given in table 1. Most of the leads (in 22 cases) emerged near the Finnish coast and only two leads were identified near the Estonian coast (Table 1). In total 14 irregular openings were identified.

Our previous modeling study [8] revealed that due to the shape of the GoF the NW winds produce the most navigable leads or openings elongated along the direction of gulf's axis. Also the N and S winds created conditions for forming leads, thus facilitating shipping through the GoF.

As estimated by Pärn and Haapala [8], the SW winds create few irregular unconnected open water areas which do not facilitate shipping in ice when the GoF is ice-covered. The S and SE winds create leads near the southern shore.

TABLE I
OCCURRENCE OF NATURAL LEADS IN THE GOF IN THE WINTER OF 2003 FROM MODIS IMAGES

Elongated leads near the Finnish coast	22 times
Elongated leads near the Estonian coast	2 times
Fully ice covered	13 times
Irregular openings of arbitrary shape	14 times

B. Observed ice data on 1971-2009 according to the EMHI ice charts. Severe winters.

In the following section we analyze historical ice cover data in the GoF during severe winters when ice cover extends over 200 000 km^2 in the Baltic. Thus, relying on the historical ice charts severe or normal winters were in 1979, 1980, 1982, 1985, 1986, 1987, 1994, 1996, 2003 and 2006. The rest were mild winters.

In severe winters when the GoF is fully ice covered the duration of ice season becomes more uniform all over the GoF. In severe winter the NW and N winds dominate. According to the modeling studies, winds from the NW and N generate leads along the GoF.

The statistical overview of lead occurrence is shown on Fig. 5. The first number shows ice days in severe winters and the second number, the occurrence of leads. In severe winters wind created leads are mostly near the Finnish coast (Fig. 5).

Ridged ice areas were identified and analyzed as well. For every ice chart the area of deformation was identified on the basis of the symbols of ridged and rafted ice. The average number of ridging days in mild and severe winters in the northern and southern part of the GoF are shown in the Table 2. In mild winters, pack ice near the northern coast was deformed 1.5 times more frequently than on the southern coast. During severe winters it is vice versa, ridges occur more frequently on the southern shore.

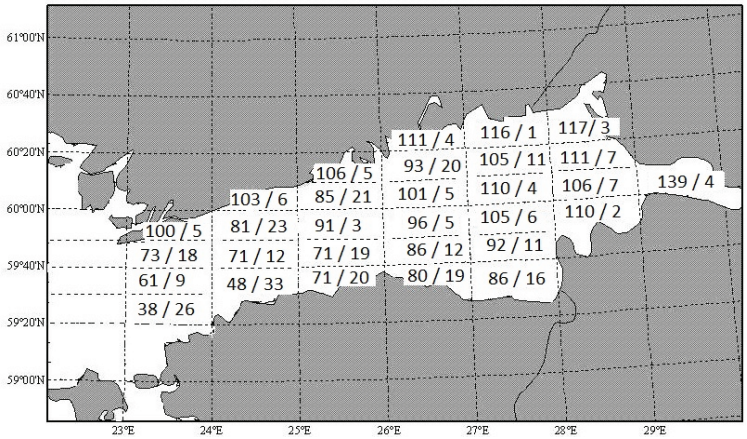

Figure 5. Average ice conditions in severe winters in the Gulf of Finland during 1971–2009 in the 1.0° longitude × 0.2° latitude grid. The first number in the cell is the average duration of ice cover in days and the second one is the occurrence of leads in days.

TABLE II
THE AVERAGE OF RIDGING DAYS DURING 1971–2009

Winter type	Northern shore	Southern shore
Mild	23	15
Severe	24	35

IV. CONCLUSIONS AND DISCUSSION

In the Gulf of Finland, the pressure from traffic is already heavy during the whole year, including the ice-covered period, and the expected economical development in the area will increase navigation in the near future. It is evident that safe and economic winter shipping in the GoF is essential for the economies of the Baltic Sea countries.

It is a complicated task (with a multiplicity of levels) to decide where to navigate in the Gulf of Finland during the ice-covered period. All off-shore operations are based on the products of monitoring and prediction of sea ice characteristics.

Traffic performance in the GoF on the one hand depends very much on the existence of the basin-size leads that facilitate navigation. On the other hand, there are a number of the ridges that are the main obstacles for safe navigation. Moreover, maritime safety depends also on compressive ice situations and extreme weather conditions like icing.

In order to examine these ice characteristics we used the ice dynamics model as well as the observed data from the MODIS satellite images and the ice charts. We detected the occurrence frequency of the leads and ridges in a number of areas of the GoF during the winters with extensive ice cover. In addition we investigated how ice deformation depends on wind speed and directions.

The analysis showed that in severe winters when the whole GoF is ice-covered elongated leads tend to occur frequently in the northern part of the gulf, but significantly more ridging occurs in the southern part. In severe winters between 1971 and 2009 approximately 35 ridging days were identified in the southern coast, whereas only 24 ridging days occurred in the northern coast. Ice deformation rate is primarily determined by the actual wind directions rather than by wind speed. The NW and also the NE–E, S winds are causing the most effective ice deformation. As demonstrated by Pärn and Haapala [8], the GoF has such a shape that mostly the NW winds create elongated openings, thus facilitating navigation through the GoF. 51 MODIS images from the winter of 2003 show that leads were occurring for almost 22 days near the Finnish coast. In severe winters, the NW winds were more common and thus there were less ice-covered days in the northern part of the GoF than in its southern part, where the occurrence of ridges is more common in severe winters.

ACNOWLEDGMENT

This study was supported by the Estonian Science Foundation (grant No. 7328 and 7633) and by the EU projects SAFEICE and SAFEWIN. We wish to thank the Estonian Meteorological and Hydrological Institute (Kai Loitjärv, Riina Vahter).

REFERENCES

[1] S. Sonninen, M. Nuutinen and T. Rosqvist, "Development Process of the Gulf of Finland Mandatory Ship Reporting System," *VTT Publications*, 2006.

[2] HELCOM "Towards a Baltic Sea with environmentally friendly maritime activities," In *2nd Stakeholder Conference on the HELCOM Baltic Sea Action Plan*, Helsinki, Finland, 6 March 2007, Web material by HELCOM, http://www.helcom.fi/stc/files/BSAP/Maritime20activities_draft20overview202007-2.pdf (accessed 25.05.2010)

[3] "SafeIce - Increasing the Safety of Icebound Shipping", http://www.tkk.fi/Units/Ship/Research/SafeIce/Public/ (accessed 25.05.2010)

[4] J. Kuronen and U. Tapaninen. "Maritime safety in the Gulf of Finland - Review on policy instruments," *Publications from the Centre for Maritime Studies*, University of Turku, 1-85, 2009http://www.merikotka.fi/safgof/Kuronen_Tapaninen_SAFGOFWP6.pdf

[5] V. Kotovirta, R. Jalonen, L. Axell, K. Riska, and R. Berglund, "A system for route optimization in ice-covered waters," Cold Regions Science and Technology, Vol. 55, pp 52-62, 2009.

[6] O. Pärn and J. Haapala, "Analysis of the ice model simulation for the Gulf of Finland in 2002/03", *Ber. Bundesamt. Seesch. Hydrogr.* 42: pp.37- 45, 2007.

[7] S. Hänninen, "Incidents and accidents in winter navigation in the Baltic Sea, winter 2002-2003," *Finnish Maritime Administration Research Report*, Helsinki, 2003, **54**, 39 pp.

[8] O. Pärn and J. Haapala, "Occurrence of synoptic flaw leads of sea ice in the Gulf of Finland," *Boreal Environment Research*, in press.

[9] .Jevrejeva, S., V.V. Drabkin, J. Kostjukov, A.A. Lebedev, M. Leppäranta, Ye.U. Mironov, N. Schmelzer and M. Sztobryn (2004) Baltic Sea ice seasons in the twentieth century. Climate Research 25, 217–227. 53.

[10] M. Leppäranta and A. Seinä, „Freezing, maximum annual ice thickness and breakup of ice on the Finnish coast during 1830–1984", *Geophysica*, Vol. 21, pp.87–104, 1985.

[11] J. Jaagus, "Trends in sea ice conditions on the Baltic Sea near the Estonian coast during the period 1949/50–2003/04 and their relationships to large-scale atmospheric circulation," *Boreal Environment Research* vol**11,** 2006, pp. 169–183.

[12] Climatological ice atlas for the Baltic Sea, Kattegat, Skagerrak and Lake Vänern (1963-1979). Swedish Meteorological and Hydrological Institute. Printed by Söfartsverkets tryckeri, Norrköping, 1982.

[13] J. Haapala, N. Lönnroth, and A. Stössel, "A numerical study of open water formation in sea ice," *J. Geophys. Res*., 2005, **110**, C9, Art. No. C09011, doi:10.1029/2003JC002200.

[14] G. Pastukhov and D. Talijev, "*Brief information on ice conditions on Gulf of Finland in the winter 2002-2003,"* NW Administration of Federal Service of Russia for Hydrometerology and Environmental Monitoring (NW Hydromet), St. Petersburg, 2003.

[15] A. Seinä, P. Eriksson, S. Kalliosaari and J. Vainio, "Ice seasons 2001-2005 in Finnish sea areas," MERI*: report series of the Finnish Institute of Marine Research*, Helsinki, 2006, **57**, 1-94.

DISSERTATIONS DEFENDED AT TALLINN UNIVERSITY OF TECHNOLOGY ON *NATURAL AND EXACT SCIENCES*

1. **Olav Kongas**. Nonlinear dynamics in modeling cardiac arrhytmias. 1998.
2. **Kalju Vanatalu**. Optimization of processes of microbial biosynthesis of isotopically labeled biomolecules and their complexes. 1999.
3. **Ahto Buldas**. An algebraic approach to the structure of graphs. 1999.
4. **Monika Drews**. A metabolic study of insect cells in batch and continuous culture: application of chemostat and turbidostat to the production of recombinant proteins. 1999.
5. **Eola Valdre**. Endothelial-specific regulation of vessel formation: role of receptor tyrosine kinases. 2000.
6. **Kalju Lott**. Doping and defect thermodynamic equilibrium in ZnS. 2000.
7. **Reet Koljak**. Novel fatty acid dioxygenases from the corals *Plexaura homomalla* and *Gersemia fruticosa.* 2001.
8. **Anne Paju**. Asymmetric oxidation of prochiral and racemic ketones by using sharpless catalyst. 2001.
9. **Marko Vendelin**. Cardiac mechanoenergetics *in silico*. 2001.
10. **Pearu Peterson**. Multi-soliton interactions and the inverse problem of wave crest. 2001.
11. **Anne Menert**. Microcalorimetry of anaerobic digestion. 2001.
12. **Toomas Tiivel**. The role of the mitochondrial outer membrane in *in vivo* regulation of respiration in normal heart and skeletal muscle cell. 2002.
13. **Olle Hints**. Ordovician scolecodonts of Estonia and neighbouring areas: taxonomy, distribution, palaeoecology, and application. 2002.
14. **Jaak Nõlvak**. Chitinozoan biostratigrapy in the Ordovician of Baltoscandia. 2002.
15. **Liivi Kluge**. On algebraic structure of pre-operad. 2002.
16. **Jaanus Lass**. Biosignal interpretation: Study of cardiac arrhytmias and electromagnetic field effects on human nervous system. 2002.
17. **Janek Peterson**. Synthesis, structural characterization and modification of PAMAM dendrimers. 2002.
18. **Merike Vaher**. Room temperature ionic liquids as background electrolyte additives in capillary electrophoresis. 2002.
19. **Valdek Mikli**. Electron microscopy and image analysis study of powdered hardmetal materials and optoelectronic thin films. 2003.

20. **Mart Viljus**. The microstructure and properties of fine-grained cermets. 2003.
21. **Signe Kask**. Identification and characterization of dairy-related *Lactobacillus.* 2003.
22. **Tiiu-Mai Laht**. Influence of microstructure of the curd on enzymatic and microbiological processes in Swiss-type cheese. 2003.
23. **Anne Kuusksalu**. 2–5A synthetase in the marine sponge *Geodia cydonium*. 2003.
24. **Sergei Bereznev**. Solar cells based on polycristalline copper-indium chalcogenides and conductive polymers. 2003.
25. **Kadri Kriis**. Asymmetric synthesis of C_2-symmetric bimorpholines and their application as chiral ligands in the transfer hydrogenation of aromatic ketones. 2004.
26. **Jekaterina Reut**. Polypyrrole coatings on conducting and insulating substracts. 2004.
27. **Sven Nõmm**. Realization and identification of discrete-time nonlinear systems. 2004.
28. **Olga Kijatkina**. Deposition of copper indium disulphide films by chemical spray pyrolysis. 2004.
29. **Gert Tamberg**. On sampling operators defined by Rogosinski, Hann and Blackman windows. 2004.
30. **Monika Übner**. Interaction of humic substances with metal cations. 2004.
31. **Kaarel Adamberg**. Growth characteristics of non-starter lactic acid bacteria from cheese. 2004.
32. **Imre Vallikivi**. Lipase-catalysed reactions of prostaglandins. 2004.
33. **Merike Peld**. Substituted apatites as sorbents for heavy metals. 2005.
34. **Vitali Syritski**. Study of synthesis and redox switching of polypyrrole and poly(3,4-ethylenedioxythiophene) by using *in-situ* techniques. 2004.
35. **Lee Põllumaa**. Evaluation of ecotoxicological effects related to oil shale industry. 2004.
36. **Riina Aav**. Synthesis of 9,11-secosterols intermediates. 2005.
37. **Andres Braunbrück**. Wave interaction in weakly inhomogeneous materials. 2005.
38. **Robert Kitt**. Generalised scale-invariance in financial time series. 2005.
39. **Juss Pavelson**. Mesoscale physical processes and the related impact on the summer nutrient fields and phytoplankton blooms in the western Gulf of Finland. 2005.
40. **Olari Ilison**. Solitons and solitary waves in media with higher order dispersive and nonlinear effects. 2005.

41. **Maksim Säkki**. Intermittency and long-range structurization of heart rate. 2005.
42. **Enli Kiipli**. Modelling seawater chemistry of the East Baltic Basin in the late Ordovician–Early Silurian. 2005.
43. **Igor Golovtsov**. Modification of conductive properties and processability of polyparaphenylene, polypyrrole and polyaniline. 2005.
44. **Katrin Laos**. Interaction between furcellaran and the globular proteins (bovine serum albumin β-lactoglobulin). 2005.
45. **Arvo Mere**. Structural and electrical properties of spray deposited copper indium disulphide films for solar cells. 2006.
46. **Sille Ehala**. Development and application of various on- and off-line analytical methods for the analysis of bioactive compounds. 2006.
47. **Maria Kulp**. Capillary electrophoretic monitoring of biochemical reaction kinetics. 2006.
48. **Anu Aaspõllu.** Proteinases from *Vipera lebetina* snake venom affecting hemostasis. 2006.
49. **Lyudmila Chekulayeva**. Photosensitized inactivation of tumor cells by porphyrins and chlorins. 2006.
50. **Merle Uudsemaa**. Quantum-chemical modeling of solvated first row transition metal ions. 2006.
51. **Tagli Pitsi**. Nutrition situation of pre-school children in Estonia from 1995 to 2004. 2006.
52. **Angela Ivask**. Luminescent recombinant sensor bacteria for the analysis of bioavailable heavy metals. 2006.
53. **Tiina Lõugas**. Study on physico-chemical properties and some bioactive compounds of sea buckthorn (*Hippophae rhamnoides* L.). 2006.
54. **Kaja Kasemets**. Effect of changing environmental conditions on the fermentative growth of Saccharomyces cerevisae S288C: auxo-accelerostat study. 2006.
55. **Ildar Nisamedtinov**. Application of ^{13}C and fluorescence labeling in metabolic studies of Saccharomyces spp. 2006.
56. **Alar Leibak**. On additive generalisation of Voronoï's theory of perfect forms over algebraic number fields. 2006.
57. **Andri Jagomägi**. Photoluminescence of chalcopyrite tellurides. 2006.
58. **Tõnu Martma**. Application of carbon isotopes to the study of the Ordovician and Silurian of the Baltic. 2006.
59. **Marit Kauk**. Chemical composition of $CuInSe_2$ monograin powders for solar cell application. 2006.

60. **Julia Kois**. Electrochemical deposition of $CuInSe_2$ thin films for photovoltaic applications. 2006.

61. **Ilona Oja Açik**. Sol-gel deposition of titanium dioxide films. 2007.

62. **Tiia Anmann**. Integrated and organized cellular bioenergetic systems in heart and brain. 2007.

63. **Katrin Trummal**. Purification, characterization and specificity studies of metalloproteinases from *Vipera lebetina* snake venom. 2007.

64. **Gennadi Lessin**. Biochemical definition of coastal zone using numerical modeling and measurement data. 2007.

65. **Enno Pais**. Inverse problems to determine non-homogeneous degenerate memory kernels in heat flow. 2007.

66. **Maria Borissova**. Capillary electrophoresis on alkylimidazolium salts. 2007.

67. **Karin Valmsen**. Prostaglandin synthesis in the coral *Plexaura homomalla*: control of prostaglandin stereochemistry at carbon 15 by cyclooxygenases. 2007.

68. **Kristjan Piirimäe**. Long-term changes of nutrient fluxes in the drainage basin of the gulf of Finland – application of the PolFlow model. 2007.

69. **Tatjana Dedova**. Chemical spray pyrolysis deposition of zinc sulfide thin films and zinc oxide nanostructured layers. 2007.

70. **Katrin Tomson**. Production of labelled recombinant proteins in fed-batch systems in *Escherichia coli*. 2007.

71. **Cecilia Sarmiento**. Suppressors of RNA silencing in plants. 2008.

72. **Vilja Mardla**. Inhibition of platelet aggregation with combination of antiplatelet agents. 2008.

73. **Maie Bachmann**. Effect of Modulated microwave radiation on human resting electroencephalographic signal. 2008.

74. **Dan Hüvonen**. Terahertz spectroscopy of low-dimensional spin systems. 2008.

75. **Ly Villo**. Stereoselective chemoenzymatic synthesis of deoxy sugar esters involving *Candida antarctica* lipase B. 2008.

76. **Johan Anton**. Technology of integrated photoelasticity for residual stress measurement in glass articles of axisymmetric shape. 2008.

77. **Olga Volobujeva**. SEM study of selenization of different thin metallic films. 2008.

78. **Artur Jõgi**. Synthesis of 4'-substituted 2,3'-dideoxynucleoside analogues. 2008.

79. **Mario Kadastik**. Doubly charged Higgs boson decays and implications on neutrino physics. 2008.

80. **Fernando Pérez-Caballero**. Carbon aerogels from 5-methylresorcinol-formaldehyde gels. 2008.

81. **Sirje Vaask**. The comparability, reproducibility and validity of Estonian food consumption surveys. 2008.

82. **Anna Menaker**. Electrosynthesized conducting polymers, polypyrrole and poly(3,4-ethylenedioxythiophene), for molecular imprinting. 2009.

83. **Lauri Ilison**. Solitons and solitary waves in hierarchical Korteweg-de Vries type systems. 2009.

84. **Kaia Ernits**. Study of In_2S_3 and ZnS thin films deposited by ultrasonic spray pyrolysis and chemical deposition. 2009.

85. **Veljo Sinivee**. Portable spectrometer for ionizing radiation "Gammamapper". 2009.

86. **Jüri Virkepu**. On Lagrange formalism for Lie theory and operadic harmonic oscillator in low dimensions. 2009.

87. **Marko Piirsoo**. Deciphering molecular basis of Schwann cell development. 2009.

88. **Kati Helmja**. Determination of phenolic compounds and their antioxidative capability in plant extracts. 2010.

89. **Merike Sõmera**. Sobemoviruses: genomic organization, potential for recombination and necessity of P1 in systemic infection. 2010.

90. **Kristjan Laes**. Preparation and impedance spectroscopy of hybrid structures based on $CuIn_3Se_5$ photoabsorber. 2010.

91. **Kristin Lippur**. Asymmetric synthesis of 2,2'-bimorpholine and its 5,5'-substituted derivatives. 2010.

92. **Merike Luman**. Dialysis dose and nutrition assessment by an optical method. 2010.

93. **Mihhail Berezovski**. Numerical simulation of wave propagation in heterogeneous and microstructured materials. 2010.

94. **Tamara Aid-Pavlidis**. Structure and regulation of BDNF gene. 2010.

95. **Olga Bragina**. The role of Sonic Hedgehog pathway in neuro- and tumorigenesis. 2010.

96. **Merle Randrüüt**. Wave propagation in microstructured solids: solitary and periodic waves. 2010.

97. **Marju Laars**. Asymmetric organocatalytic Michael and aldol reactions mediated by cyclic amines. 2010.

98. **Maarja Grossberg**. Optical properties of multinary semiconductor compounds for photovoltaic applications. 2010.

99. **Alla Maloverjan**. Vertebrate homologues of Drosophila fused kinase and their role in Sonic Hedgehog signalling pathway. 2010.

100. **Priit Pruunsild**. Neuronal Activity-Dependent Transcription Factors and Regulation of Human *BDNF* Gene. 2010.

101. **Tatjana Knazeva**. New Approaches in Capillary Electrophoresis for Separation and Study of Proteins. 2011.

102. **Atanas Katerski**. Chemical Composition of Sprayed Copper Indium Disulfide Films for Nanostructured Solar Cells. 2011.

103. **Kristi Timmo.** Formation of Properties of $CuInSe_2$ and $Cu_2ZnSn(S,Se)_4$ Monograin Powders Synthesized in Molten KI. 2011.

104. **Kert Tamm**. Wave Propagation and Interaction in Mindlin-Type Microstructured Solids: Numerical Simulation. 2011.
105. **Adrian Popp**. Ordovician Proetid Trilobites in Baltoscandia and Germany. 2011.